ADDITION OF CONDENSABLE OR NON-CONDENSABLE GAS TO STEAMFLOOD PROCESSES FOR IMPROVED HEAVY OIL RECOVERY BY GRAVITY DRAINAGE

A REPORT SUBMITTED TO THE DEPARTMENT OF ENERGY RESOURCES ENGINEERING

OF STANFORD UNIVERSITY

IN PARTIAL FULFILLMENT OF THE REQUIREMENTS FOR THE DEGREE OF MASTER OF SCIENCE

By
Khalid Rashid Alnoaimi
August 2010

I certify that I have read this report and that in my opinion it is fully adequate, in scope and in quality, as partial fulfillment of the degree of Master of Science in [Energy Resources] [Petroleum] Engineering.

_____

Prof. Anthony Kovscek
(Principal Advisor)

I certify that I have read this report and that in my opinion it is fully adequate, in scope and in quality, as partial fulfillment of the degree of Master of Science in [Energy Resources] [Petroleum] Engineering.

_____

Dr. Louis Castanier

Abstract

This research focused on quantifying the advantages of adding condensable and non-condensable gases to steamflooding for heavy-oil recovery governed by gravity drainage in naturally fractured carbonate reservoirs. The work consists of numerical and immature physical modeling. The numerical modeling investigates the effects of gas addition on recovery through a series of sensitivity studies in order to develop a clear behavior prediction of the roles the gases play on recovery. The numerical investigation proceeds, afterwards, to include the construction of two synthetic models that mimic actual rock properties for two physical core plugs used in the laboratory. The first model has a short length of 3.5 inches, prototype model, and the second model has a long length of 28 inches. The development of both models in the numerical analysis is made by a thermal reservoir simulator, STARS CMG©. The numerical results compare between the three injection schemes, steam, steam/N_2 and steam/CO_2, and between the recovery behavior of the prototype and original experiments. The work, also, sheds light on the physical aspects of the study. This includes the modeling and preparation of the short and long core plugs in the laboratory.

The research work concluded that, numerically, the addition of non-condensable gas to steamflood processes increases the cumulative oil recovery slightly over steam injection but more importantly accelerates oil production at early time of the process. The injection of condensable gas accelerates the production to some extent at early time of production but the rate drops afterwards. The cumulative oil recovered by the co-injection of condensable gas is slightly less than steam alone injection. The main differences between the two gases are attributed to the solubility factor of CO_2 in oil and water phases and the better steam propagation profile in the N_2 injection case.

Acknowledgments

In the name of holly Allah, Most Gracious, Most Merciful

I express my deep appreciation to my research and academic advisor Prof. Anthony Kovscek for his masterful insights and guidance during the course of my work in Stanford. This work would not have been possible without his support.

The appreciation is extended to Dr. Louis Castanier who inspired me with ideas and experimental designs and who had many valuable comments during the affiliates meeting. I also cannot forget my dear lab partner Dr. Elliot Kim for his unyielding support during my whole period of work in the lab. His instructions and hand help were very supportive for my work.

I am also grateful for all my sponsors, SUPRI-A group for funding this research and for Saudi Aramco for funding my tuition.

Thank you for all the faculty members, staff and students of the energy resource engineering department for making the educational environment fun and interesting.

Special thanks to my friend and Aramco mentor Dr. Ghaithan Almontasheri for teaching me the fundamentals of research and directing my ambitions toward research work.

At the end, I would like to thank my dear wife Maha for being so patient on me during my busy days and cold nights. This work is dedicated to her and to my son Rashid who I missed during the time of writing this documentation. I also want to thank my dear parents for their continuous prays for me and emotional support.

It is an honor and pleasure to be a member at this respected group.

Khalid Alnoaimi

Contents

List of Tables

List of Figures

Chapter 1

1. Introduction

Steamflooding of oil reservoirs is the most effective EOR method to date as gauged by cumulative oil recovery. It is primarily associated with heavy-oil recovery and is emerging as a solution for improved recovery in fractured systems. Steamflooding is less affected negatively by gravity than waterflooding, and therefore, potentially yields a better injection profile throughout the reservoir. However, one noticeable drawback of steam injection stems from the early channeling of steam under the cap rock to the producer well, establishing a path for the following steam to chase. This early breakthrough reduces the average oil saturation in the reservoir leading to a lower cumulative oil recovery. One theoretical solution to overcome this problem is by introducing a non-condensable gas such as nitrogen to the steamflooding process. The aim of injecting the non-condensable gas is to form a gas drive that offers additional sweep in the reservoir and to increase the oil volume in place as the gas dissolves in the oil. It also carries the heat to the production well faster than steam allowing heating for longer periods of time and thus reducing further oil viscosity. Not only heat, but even pressure is carried along by the non-condensable gas to the producer ahead of the steam forming the gas drive solution. Theoretically, the simultaneous injection of non-condensable gases has shown promising results of increased oil recovery compared with steam alone injection in oil wells (Bagci and Gumrah, 2004). Further details are presented in literature review section.

The objective of this research work is to study the effects of co-injecting non-condensable gases such as nitrogen during steamflooding and compare them with the effects of co-injecting condensable gases such as soluble carbon dioxide in order to improve heavy-oil recovery by steamflooding in fractured reservoirs. The study starts with a literature review, followed by conception of steam/gas gravity drainage. After that, a clear definition of the problem statement is introduced. Next, approaches to the solutions are proposed, numerical and physical modeling, and tailed by sensitivity studies that shape the experimental conditions in both models and provide preliminary conclusions. Results, after that, are divided into simulation and experimental phases and only results of the simulation study are presented and discussed. The experimental phase, except for one experiment, is considered future work, but the laboratory work is presented. Finally, a brief conclusion that summarizes the findings is presented and followed by future work.

1.1. Literature Review

The concept of injecting non-condensable gases during steamflooding oil recovery started in the early 1970s and became even more popular with the advent of reservoir simulation. In most cases, as will be discussed, it was found that the addition of non-condensable gases, CO_2 in particular, causes a noticeable increase in oil recovery for different API gravities. The improvements in some of the studies exceeded 50% of OOIP in a laboratory scale.

Pursley performed air, CH_4, and CO_2 injection with steam stimulation in a 1-D laboratory model experiment. The objective of the experiment was to measure the effects of co-injecting the gasses with steam on improving the oil/steam ratio. Remarkably, the improvement of oil recovered was noticeably greater for air and CH_4 but not for CO_2 (Pursley, 1975).

A few years later, Redford conducted a 3-D laboratory model experiment to study the effects of CO_2/steam or CH_4/steam injection on oil recovery of Athabasca tar. Redford found a noticeable improvement of oil recovery with both injection mixtures. This increase was attributed to a solution gas-drive mechanism (Redford, 1982).

In the same year, a numerical study by Louis Leung (1982) showed that the major contributor of increased recovery was the viscosity reduction effect of CO_2 on heavy-oil in high compressibility reservoirs. The effect of solution gas of the injected CO_2 rises in a normal compressibility reservoir where the oil recovery becomes more advantageous over steam alone injection when the solubility of CO_2 in water is ignored. The addition of CO_2, however, during steam flood increases the recovery by only a small amount but the production rate is accelerated before steam breakthrough by the solution of CO_2 in the oil. The study also noticed that the swelling effect of CO_2 does not appear to be important in increasing the recovery since the effect is small at high temperature when compared with the thermal viscosity reduction and expansion of the oil (Leung, 1982).

Hutchinson et al. (1983) studied the co-injection of steam and nitrogen, carbon dioxide or air at low pressures into Utah tar sands. It was observed that the addition of the non-condensable gases gives only a slight improvement in oil recovery compared to steam injection alone (Hutchinson, lp, Shirazi, 1983).

Using a linear physical model, T.G. Harding et al. (1983) investigated the performance of steamflood in the presence of carbon dioxide and nitrogen on moderately viscous refined oil. The findings were similar to previous authors', in that the total oil recovery was improved slightly by the addition of the gases and the oil production rate was considerably accelerated before steam breakthrough. They attributed these results to the additional gas drive supplied by the non-condensable gases (Harding T. G., et. al., 1983).

Hong and Ault (1984) used a compositional steam injection simulator to study the effects of CO_2 injection on oil recovery by steamflooding for light and heavy-oil reservoirs. The

heavy-oil reservoir was characterized by a depth of 1,000 ft, a permeability of 4,000 mD, a porosity of 34.2% and a thickness of 100 ft. On the other hand, the light oil reservoir had a depth of 2,500 ft, a permeability of 40 mD, a porosity of 32% and a similar thickness of 100 ft. In both reservoirs the vertical permeability was assumed to be 50% of the horizontal permeability. A homogenous formation was also assumed for both reservoirs. The results showed that in heavy-oil reservoirs the role of CO_2 in steam injection was a significant acceleration of the production in the early life of the project. However, the cumulative recovery over the project life was found to be the same as that obtained by steam alone. The early increase in the production was attributed to the improved sweep of the reservoir by the injected CO_2. Similarly, for the light-oil reservoir it was found that CO_2 accelerates the oil production due to the increase in the volume of the displacing gas phase. There was, however, a slight increase (6 to 7%) in the oil recovered at the end of the project life. This was attributed to the enhanced steam distillation and the lowering of the oil viscosity by CO_2 dissolution in the oil (Hong and Ault, 1984).

Hornbrook et al., (1989) studied the effects of CO_2 addition to steam on recovery of West Sak crude oil. They found the simultaneous injection of CO_2 and steam beneficial in recovering more oil than steam alone injection using 1-D laboratory displacement study. The major conclusions were that the addition of CO_2 during steam flood increases the recovery rate and improves recovery by 14.8% over conventional steamflooding after 6 PV of steam injection. In addition, the optimum CO_2/steam molar ratio found for maximizing the recovery was 1:3. They also found that adding CO_2 to steam at the same temperature will increase the yield for the same amount of water distilled and that the addition of CO_2 at greater temperatures causes significant swelling in the oil phase that should enhance the oil recovery (Hornbrook et. al., 1989).

Exploring the role of non-condensable gases in SAGD process, Canbolat S., et al. 2004 studied the non-condensable gases effect on improving the recovery of heavy-oil using physical modeling. As the fraction of CO_2 added increases, the paper claims, the steam condensation temperature and the steam-oil ratio decreases. This makes the oil less mobile and, therefore, the cumulative oil recovery and rate were decreased accordingly and independently of well separation as long as no initial non-condensable gas existed in the reservoir (Canbolat S., et al., 2004).

Bagci and Gumrah (2004) conducted 1-D cylindrical tube and 3-D rectangular box physical model experiments to assess the effects of injecting CO_2 and CH_4 on the recovery of heavy-oil mixed with unconsolidated limestone by steamflooding. The results showed that the optimum gas/steam ratio that maximized the recovery in the 1-D model was about 9.4 cm^3/cm^3 for both CO_2/steam and CH_4/steam injections while for the 3-D model the ratio dropped to 8.7 cm^3/cm^3 for CH_4/steam and remained the same for CO_2/steam. It was also found for the 1-D model that at 1.5 PVI of steam; the oil recovery of CO_2/steam was 66.5% of OOIP and 60.4% of OOIP for injected CH_4/steam, compared with 50.9% of OOIP for steam alone. The 3-D model, however, had lower values where the oil recovery of CO_2/steam system was 36.2% of OOIP and 49.9% for CH_4/steam

injection compared to 21.7% for steam alone. It was noticed by them that the injected non-condensable gas formed a permanent gas phase across the top of the model. While this gas layer reduced heat losses to the overburden, the heat reached the producing well earlier in comparison to steam alone test. It was also noticed that there was a temperature depression of steam due to the presence of non-condensable gas (Bagci and Gumrah, 2004).

The presented study in this research work is neither a cyclic steam nor a SAGD processes but steamflood governed by gravity drainage process. Therefore, the role of non-condensable gases on improving heavy-oil recovery in naturally fractured reservoirs is still an open question and worth investigating.

The chief goal of initiating this research work is to develop a sufficient understanding of how non-condensable gases such as nitrogen and condensable gases such as soluble carbon dioxide can improve oil recovery during a steamflooding process governed by gravity drainage in fractured wells with low matrix permeability. Therefore, introducing brief backgrounds about steamflood, steam/non-condensable flood, steam/condensable processes and gravity drainage is appropriate.

1.2. Gravity Drainage Concept

Gravity drainage is a useful mechanism that is used when recovering heavy-oil. When the heavy-oil is heated by the steam temperature, the high viscosity of the oil decreases to a lower value. This improves the oil mobility and makes it more susceptible to gravity influence and, therefore, the oil drains to the producer wells smoothly. The concept of a gravity drainage process in this study is different from the steam-assisted gravity drainage in that steam is forced, in this study, to enter the formation using vertical injectors and oil is collected at the bottom by the producers. Furthermore, SAGD is usually used in sandstone reservoirs where high permeability is key factor unlike the adopted concept presented here where steam enters very tight formation, < 1mD. The gravity drainage is supported by steamflood process with minimal pressure drop across the cores to allow the gravity effect to dominate oil recovery.

There have been many gravity drainage models proposed in literature about one of that is the "Gravity Drainage Theory" by (Cardwell et al., 1948). This section discusses this proposed concept for the process used in this study to be understood.

When looking at Figure 1-1, curve A is what a liquid distribution looks like when vertical column of porous medium is saturated with that liquid given that the top and bottom of the column are opened. In this case the liquid is allowed to drain. The column lower end is 100% saturated. Above the fully saturated region is a gradual decreasing saturation above that a region of constant saturation exists. Such a curve is known as the equilibrium drainage curve that is curve A. The drainage process is represented in this figure. If there is another liquid saturation distribution in the column, for example curve B, then the distribution appears to be unstable and tends to change until it reaches the stability level as indicated in curve A. In fact, this is a natural conclusion in that curve B

becomes curve A through the relative motion of parts of the liquid body. This motion is governed by Darcy law.

Darcy's law is expressed as,

$$v = \frac{k}{\mu}\rho g - \frac{k}{\mu}\frac{\partial p}{\partial z} \qquad \textbf{(1-1)}$$

where v is the macroscopic fluid velocity downward, k is the effective permeability of the medium to the fluid, μ is the fluid viscosity, ρ is the fluid density, g is the gravity acceleration and p is the fluid pressure.

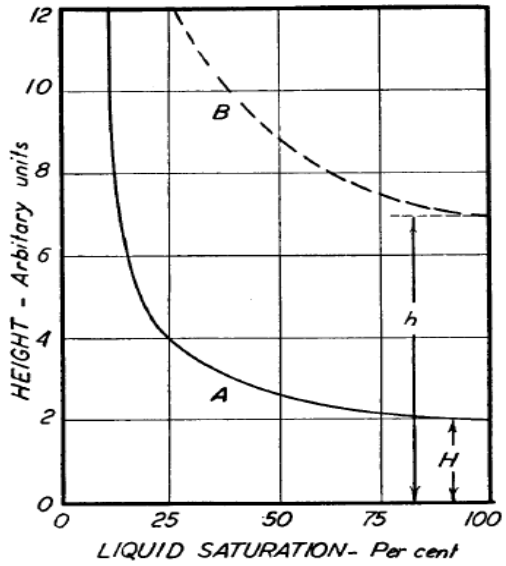

Figure 1-1: Liquid saturation versus height (Cardwell et al., 1948).

Several Conclusions can be drawn from Equation 1-1. First, the effective permeability is a function of the fluid saturation, i.e. as the permeability increases, the fluid saturation increases and vice versa. Second, the fluid pressure has two variations with fluid saturation. One in the partially saturated region, before the 100% region in the column and second in the fully saturated region. In the first region, partially saturated, seven units above on curve B the variation of fluid pressure is a function of fluid saturation, i.e. as the pressure decreases the saturation decreases. In accordance with the capillary behavior, the liquid pressure gradient becomes a function of the saturation gradient alone only if part of the pore spaces that are not filled with liquid is filled with gas having negligible vertical pressure gradient. In the fully saturated region, no saturation gradient exists and so no pressure gradient as well. If the column is still open from top and bottom, and the vertical pressure gradient of the gas surrounding the column is negligible, then the externally applied pressure must be equal at both ends of the column. In such a condition, the velocity of the fluid becomes zero. If this value is substituted in Equation 1-1 for the velocity, the pressure gradient in the 100% region of saturation becomes the following:

$$\frac{\partial p}{\partial z} = \rho g \qquad \textbf{(1-2)}$$

This is different from the analysis discussed previously about the pressure saturation at the 100% region of saturation. This is probably due to the fact that at the upper boundary of the 100% saturation region the liquid pressure is different from the gas pressure. According to the same reference, furthermore, experiments showed and discussed the existence of a definite interfacial curvature between liquid and gas at that boundary and thus pressure drop exists across the interface. Back to curve A, if the top part of the fully saturated region has a height of *H*, then the negative pressure would have a magnitude of ρgH . Therefore, the pressure gradient in the fully saturated region becomes:

$$\frac{\partial p}{\partial z} = \rho g \frac{H}{h} \qquad \textbf{(1-3)}$$

Where *H* is the height of the top of the 100% saturated region after reaching equilibrium and *h* is the same before reaching the equilibrium.

In conclusion, two special equations can be derived from Darcy's law. One is for the partially saturated region, Equation 1-4, and second for the fully saturated region, Equation 1-5.

$$v_u = \frac{k}{\mu}\rho g - \frac{k}{\mu}\frac{\partial p}{\partial z} = \frac{k}{\mu}\left(\rho g - \frac{\partial p}{\partial \xi}\frac{\partial \xi}{\partial z}\right) \qquad \textbf{(1-4)}$$

Where v_u is the velocity in the partially saturated region and ξ is the fractional saturation, the variable upon that the pressure, *p*, depends.

$$v_s = \frac{k}{\mu}\left(\rho g - \rho g \frac{H}{h}\right) = \frac{k\rho g}{\mu}\left(1 - \frac{H}{h}\right) \qquad \textbf{(1-5)}$$

Where v_s is the velocity in the fully saturated region.

The analytical solution proceeds to further details. In his book, however, Butler (1991) derived an expression from the presented analysis that captures the change of fluid saturation, oil in this case, as a function of drainage height during gravity drainage. This equation is,

$$\overline{S}_{or} = 0.43\left(\frac{v_s \phi h}{kgt}\right)^{0.4} \qquad \textbf{(1-6)}$$

Where S_{or} is the average residual oil saturation after time t, h is the maximum drainage height, k is the absolute permeability, v_s is the kinematic viscosity of the oil at steam temperature, φ is the porosity and g is the gravity acceleration.

1.3. Steamflooding Process

During the steamflooding process, steam is forced to enter continuously the rock from injection wells and oil is displaced to separate production wells. The areas around the injectors become heated to steam temperature and they expand toward the production wells.

With viscous oil in the formation, steam tends to override because of its low density to top zones providing heat. The propagation of steam into the formation causes the temperature of the oil to increase and the viscosity to decrease. This mitigates the oil mobility and allows it to drain toward the production wells. As the steam starts penetrating, however, through the formation, it loses some heat to the rocks by conduction causing the gas phase to drop to condensate, shown in Figure 1-2. The condensation takes place ahead of the advancing steam zone where a region of hot water is formed and acts as a hot water flood (Butler, 1991). Such a profile occurs when steam is injected non-isothermally into the reservoirs. Therefore, as the steam temperature decreases, the heat provided to the system decreases as well. This reduction in heat slows the decrease in the oil viscosity, hence the thermal efficiency of the process decreases and so the oil production. If additional steam volumes are injected for longer periods of time, the steam zone would expand together with the area below and above. This would, however, increase the heat lost to the surrounding overburden/underburden and only of little portion of the heat is useful in heating up the reservoir (Butler, 1991). The zones around the injection wells become heated to the saturation temperature of the steam, and these zones expand toward the production wells. This is why generally steamflooding technique is suitable for shallow reservoirs (Moussine et al., 2007). Therefore, heat control during steamflood is of a great importance to keep the process efficient and economically justifiable.

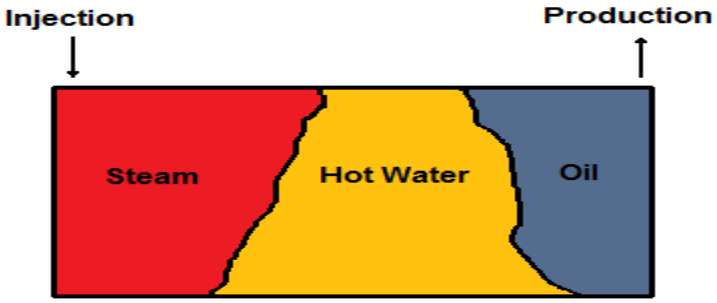

Figure 1-2: Steam injection profile.

1.4. Steam/Gas Flooding Process

Several studies, in the literature review section, have shown that simultaneous injection of steam and gas may or may not improve the cumulative recovery of heavy-oil. It was concluded for the most part that the addition of gases accelerates the oil production rate at the early life of production and that the oil recovery if not increased will be about the same at lower steam temperature. Such observations instigate the curiosity of studying the physics and thermodynamic states of the addition of such gases to steamflood processes. The following section discusses two types of co-injected gases, non-condensable, such as nitrogen, and condensable gases such as soluble carbon dioxide.

1.4.1. Condensable and Non-Condensable Gases

Condensable gases are the types of gases that are soluble in a liquid phase while the non-condensable gases are almost insoluble in liquid phase. For example, at 500 psia and 100^{o}F, the K-value of nitrogen is 30 while for carbon dioxide is 3.5 (Harding T. G., et. al., 1983). Therefore, the condensable gas forms a gas in solution drive that causes the swelling of oil, i.e. increases the volume of oil in place, that creates more mobile oil that can be produced after decreasing its viscosity. The condensable gas, in this study, is assumed to exist in water and oil phase while the non-condensable gas does not dissolve in either phase.

During steam/gas simultaneous injection, it is favored to keep the steam temperature constant for as long as possible to allow more heating for longer periods of time. The role of the co-injected gas comes into play in supporting steam pressure and temperature. The gas carries the heat and pressure ahead of the steam to the producer well (Aherne and Birrell, 2002). This creates a gas drive that distributes heat and pressure across the reservoir that increases the thermal efficiency of the process, hence reducing further the oil viscosity. This effect also improves the sweep efficiency and adds more pressure gradient to the reservoir forcing more oil to the producer well (Clampitt et al., 1991).

The thermodynamics of steam/gas system is of a great importance in this study. When the gas is added to steam adiabatically at the same pressure and temperature, it decreases the temperature of steam. The reason is the lowering of the steam partial pressure, in the vapor phase, as a result of adding the gas isobarically. This decrease in the steam pressure allows the liquid phase water to vaporize increasing the steam quality. The decrease in pressure also means an increase in steam volume that provides additional sweep of the reservoir. Furthermore, the decrease of steam temperature reduces the heat lost to the surrounding overburden/underburden (Hong and Ault, 1984). According to the study conducted by Hong and Ault (1984), however, CO_2 addition increased the system total pressure that compensates for the decrease in the steam partial pressure. It was also found that the temperature of the steam zone increased beyond injecting steam alone.

When co-injecting gas in a steamflood process, it is expected that the gas rises to the top of the reservoir very quickly and reaches the top long before the upper parts are heated. After that, the gas spreads along the upper portion of the reservoir and forms a very thin

layer (Butler et al., 1999). This is attributed to the fingering process made by the gas when rising to the top section. During this process the gas displaces very little portions of the oil counter-currently but as mentioned previously it carries pressure to the upper parts as well, shown in Figure 1-3. A mathematical analysis implemented by (Butler et al., 1999) showed that when the gas fingers upwards the pressure at the top of the reservoir is almost equal to the pressure at the bottom parts. The importance of this is that the oil would drain, therefore, by the potential gradient $\Delta\rho g$ and the gas would fill the emptied volumes.

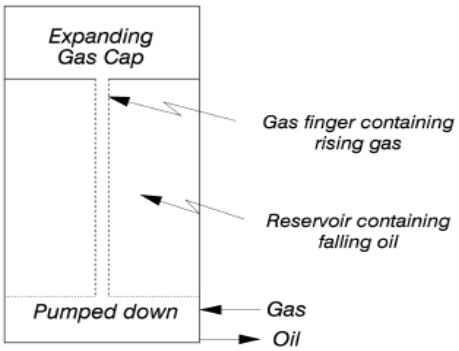

Figure 1-3: Non-condensable gas fingering (Butler et al., 1999).

1.5. Isothermal Flood vs. Non-Isothermal Flood

This section discusses two different steam delivery processes: isothermal and non-isothermal injections. The reason for introducing the two delivery schemes is to study how the co-injected gases would affect oil recovery by gravity as well as to justify the intended work toward isothermal process in the experimental analysis in later research work when using long core in flooding experiments. The following paragraphs give a brief description about each process inspired from (Lake 1989).

1.5.1. Theoretical Background

A non-isothermal steam injection process occurs when steam is injected at a high temperature into a formation with lower temperature. The steam dissipates heat into the formation by conduction. The heat, as a result, is carried to the rocks and reaches the oil faster than the steam does. This is, in fact, the advantage of injecting steam into a thick carbonate formation where the heat transfer rate by conduction is high.

In an isothermal process no condensation of steam takes place when the porous medium is heated initially to steam temperature. Therefore, no hot water front is formed during the injection and no heat is lost to surrounding medium. A typical propagation profile is depicted in Figure 1-4.

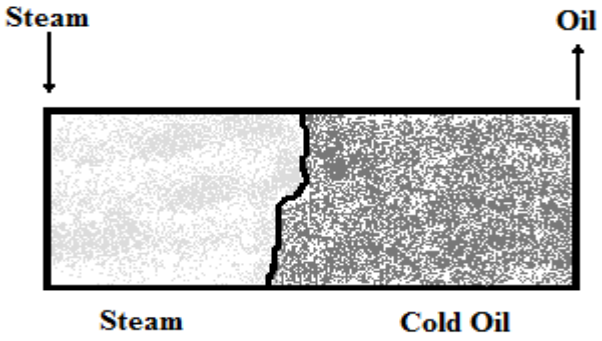

Figure 1-4: Isothermal steam injection.

As the steam enters the formation at high constant pressure, it starts displacing oil in three steps: one that is contacting the oil, two is heating and reducing oil viscosity and three is driving the heated oil away to the wellbores by pressure drop and gravity effect. During the displacement process no mixing occurs between the displacing and displaced fluids and therefore no issues with miscibility nor with stability. The displacement process runs under constant injection and production pressures, and constant temperature throughout the medium.

Steam flow, in an isothermal process, is quantified by Darcy's equation. In this study, the injection profile is in the k-direction that is pointing downward and for such a scheme the Darcy velocity is given as:

$$\overrightarrow{u_k} = -\lambda_{rk}\,\vec{k}.(\vec{\nabla}P_k + \rho_k\,\vec{g}) \tag{7}$$

where $\overrightarrow{u_k}$ is the Darcy velocity in k direction, $\vec{k}$ is the permeability tensor, $\vec{\nabla}$ is the divergence operator, λ_{rk} is the mobility ratio of k phase, P_k is the pressure of phase k, ρ_k is the density of phase k, and g is the gravity acceleration.

The Darcy equation is used to calculate the steam propagation velocity in the formation. The average steam velocity, interstitial steam front velocity, is calculated then for a one dimensional system as:

$$v = \frac{u_{steam}}{\phi} \tag{8}$$

where v is the interstitial steam front velocity, u_{steam} is the steam Darcy velocity, and φ is the formation porosity.

1.6. Dimensionless Analysis

To capture the mechanism of steam flow displacement in a reservoir during a thermal recovery process, it is essential to introduce the concept of dimensionless analysis. The importance of dimensionless analysis rises from the ability to determine the balance between the different forces exerted on a sample core, capillary, viscous and buoyancy

forces, that translate fluids displacement patterns in the multiphase porous system. For example, if the ratio of gravity to capillary forces is large, the displacement pattern is said to be governed by gravity.

This section defines briefly the interchange effects of these forces quantitatively and emphasizes their effects on oil recovery. There are several dimensionless groups that are necessary in this study such as capillary number, N_C, and Bond number, N_B. The capillary number is defined as the ratio of viscous force to capillary force. If the capillary number is small, then capillarity dominates the flowing regime at the pore scale. The Bond number is defined as the ratio of Buoyancy force to capillary force. If the buoyancy force, i.e. gravity force, is larger than capillary force, then the flow pattern is influenced by gravity. The following two equations define the capillary and Bond numbers:

$$N_C = \frac{Viscous\ Force}{Capillary\ Force} = \frac{v\mu}{\sigma} \tag{9}$$

where v is the Darcy velocity, μ is the viscosity of displacing phase, and σ is the interfacial tension between the displacing and displaced fluids.

$$N_B = \frac{Buoyancy\ Force}{Capillary\ Force} = \frac{\Delta\rho g l^2}{\sigma} \tag{10}$$

Above $\Delta\rho$ is the density difference between the two fluids, g is the gravitational constant, l is the characteristic length of the porous medium, taken as average grain radius, (Grattoni et al, 2001).

These two equations are used to determine the Bond and capillary numbers for the non-isothermal steam injection process. In isothermal injection processes, steam condensation is negligible when the temperature of the core is the same as or close to steam temperature. This affects the displacement flow pattern to be three phase flow system and for such a system the Bond and capillary numbers become, Equations 11 and 12.

$$N_B = \frac{\Delta\rho_{og} gZRa}{2\sigma_{go}} \qquad \text{(C.A. Grattoni et al., 2001)} \tag{11}$$

Where $\Delta\rho_{og}$ is the difference between steam and oil densities, Ra is the average pore throat radius, Z is the average position of the gas interface and σ_{go} is the interfacial tension between the steam and oil. On the same hand, the capillary number is given by:

$$N_C = \frac{2v_g \mu_g}{Pc_{go} Ra} \qquad \text{(C.A. Grattoni et al., 2001)} \tag{12}$$

Equipment has been designed by Elliot Kim for the sake of measuring the Bond and capillary numbers in the lab between the oil interface and steam statically, Figure 1-5. No data, however, are available in this study yet about the dimensionless numbers but this will take place in the next phase.

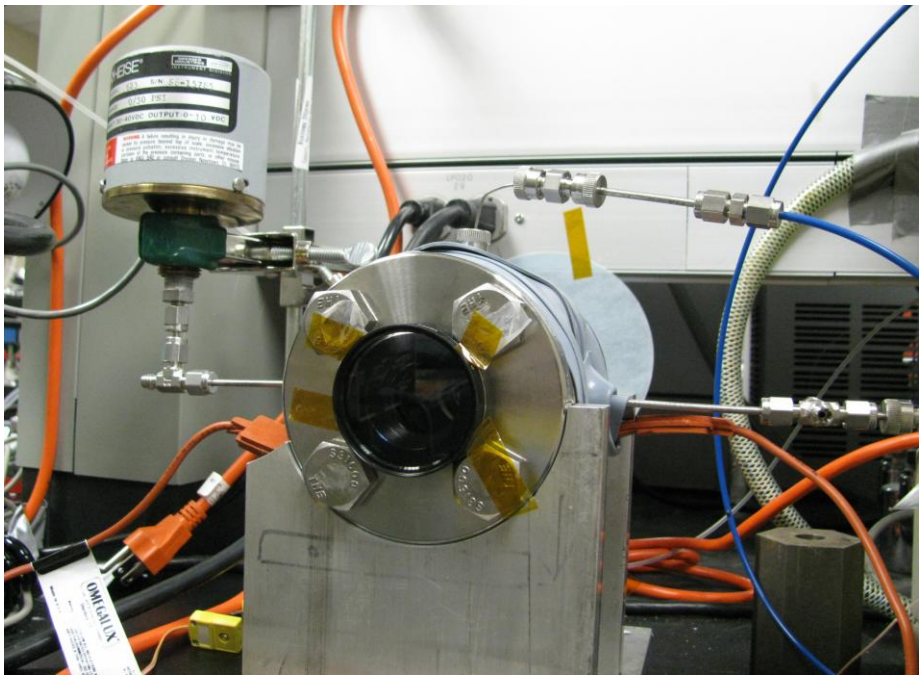

Figure 1-5: Steam-oil interfacial measurement equipment.

1.7. Problem Statement and Description

Butler (1991) explained extensively about the steam-assisted gravity drainage concept and since then there have been many publications that explored the effects of co-injection of non-condensable gases during SAGD process such as (Canbolat et al., 2004). The conclusions, for most cases, ranged between none to slight oil recovery improvements. Furthermore, some studies showed that co-injecting non-condensable gases during steamflooding processes is usually advantageous over steam alone injection. There were few very optimistic studies such as the one presented by Bagci and Gumrah (2004) in that more than 60% of oil originally in place was recovered using 1-D and 3-D physical models for steam/CO_2 and steam/CH_4 injections. The majority of the studies presented in the literature review section agreed upon a main advantage that is the acceleration of the oil production rate at the early life of the process. It is important, however, to mention that most of the studies of co-injecting gases were made on SAGD or steam cyclic processes. This study explores vertical steamflood injection by gravity drainage effect. It is quite interesting to observe how the co-injection gases behave in such processes.

The study presented in this research work focuses on the effects of co-injection of nitrogen with steam as non-condensable gas and carbon dioxide as condensable gas on heavy-oil recovery governed by gravity drainage process using steamflooding. The study investigates the physics observed during steam/gas co-injection process when gravity drainage is the main mechanism of production, that is, small pressure drop across the

system. The study uses two synthetic cores with different lengths for the purpose of investigation. One with shorter length of 3.5 inches, prototype experiment, and another with longer length of 28 inches, original experiment. It is expected that the long core will be more susceptible to gravity influence than the shorter core. Yet, the effects of co-injecting steam with condensable and non-condensable gases on gravity are to be thoroughly studied for heavy-oil in naturally fractured formations with tight matrix permeability and results from the physical and numerical modeling must show similar trends before casting solid conclusions on this subject. Nonetheless, this work only presents simulation analysis of the indicated processes. The analysis uses a thermal reservoir simulator, STARS from CMG to do the study. The study also sheds the light on some experimental work that will continue after this documentation to catch any possible agreement between the two modeling.

Chapter 2

2. Approaches to Solution

2.1 Numerical Analysis Description

The numerical analysis in this research work investigates the effects of steam/gas simultaneous injection on a heavy-oil recovery process governed by gravity drainage in naturally fractured carbonate reservoirs. It also compares the effects of co-injecting CO_2 and N_2 with steam on the recovery trend. Therefore, two processes have been studied for this purpose, prototype and original experiments. The prototype experiment consists of a short core simulated rock with a length of about 3.5 inches, 8.9 cm. The original experiment, on the other hand, consists of a long core simulated rock with a length of about 28 inches, 71 cm. The difference in length is a telling factor of how gravity influence responds to the gas co-injection effects on oil recovery. The type of rocks used is a naturally fractured carbonate with vuggs. The cores have low petro-physical properties. Further details about the core types and specifications are mentioned in the experimental description. The simulation analysis uses some of the measured rock properties during the laboratory work and incorporates them in the model. This includes the oil type and viscosity used in the model. There are, however, many sources of uncertainty with using the simulation model. Nevertheless, the intention is to present a healthy numerical study and in a later research work implement the two experiments physically to come up with valid history match data. Until then, both processes are assumed to capture the nature of field rocks. Each process is discussed in the following sections.

2.2 Experimental Analysis Description

The experimental analysis focuses on developing coreflood experiments for two cores with the same lengths indicated in the numerical analysis. The cores are carbonate type brought from naturally fractured reservoirs. It is intended to perform three experiments on the prototype core and two on the original cores. The prototype experiment includes steam alone, steam/CO_2, and steam/N_2 experiments while the original includes only steam alone and steam/N_2 experiments. This work, however, presents only the steam alone experiment performed on prototype core. The rest of experiments will take place afterwards. More details are found in the *Experimental Modeling Section*.

Chapter 3

3. Sensitivity Analysis

This section presents an extensive sensitivity analysis performed on a base case model in order to determine the effects of inputs and modeling parameters before conducting the original simulation study reported in this documentation. The analysis is intended to assess identifying important parameters and in quantifying effects of uncertain parameters on results. The intended parameters to be studied are: oil gravity, gas concentration and effects of steam temperature and partial pressure during gas injection.

3.1. Base Case Model

The sensitivity study uses a base case model that has different inputs from the original experiments. The following paragraphs briefly introduce the inputs.

3.1.1. Oil Viscosity

The oil used in the study is a field crude and has a gravity of 14^{o}API with a highly viscous nature. Figure 3-1 shows the oil viscosity as a function of temperature. At a temperature of 150^{0} F, the oil viscosity is about 945cp.

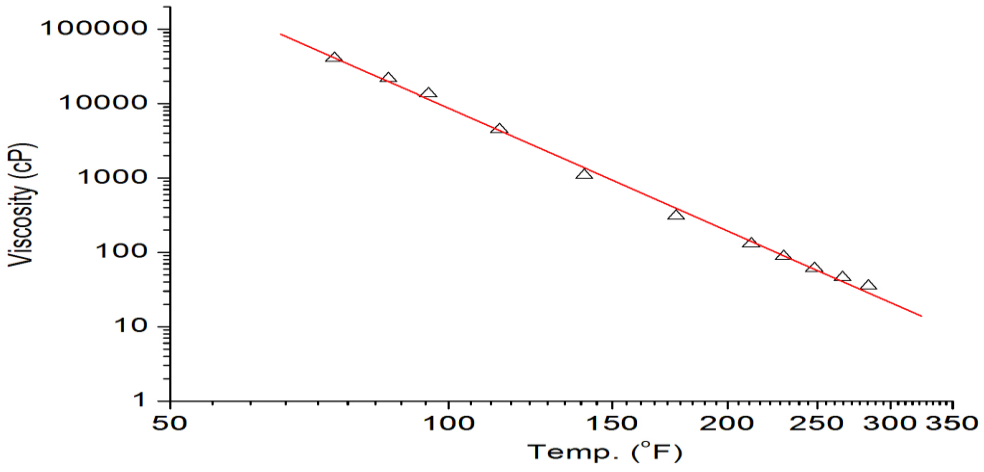

Figure 3-1: Oil viscosity-temperature curve.

3.1.2. Grid System

The gridding system used in the base case of the sensitivity analysis model is homogeneous, 2-D Cartesian model with gravity drainage option and capillary pressure

effects. The model consists of matrix with three fully extended fractures on the center and sides of the model. The fractures are modeled with fine grid style. The injection wells are located at the top while the production wells at the bottom. The pressure distribution in the model is hydrostatic. This is obtained by choosing the vertical equilibrium option in the simulator. The grid model is given in Figure 3-2. The Grid properties are found in Table 3-1-1.

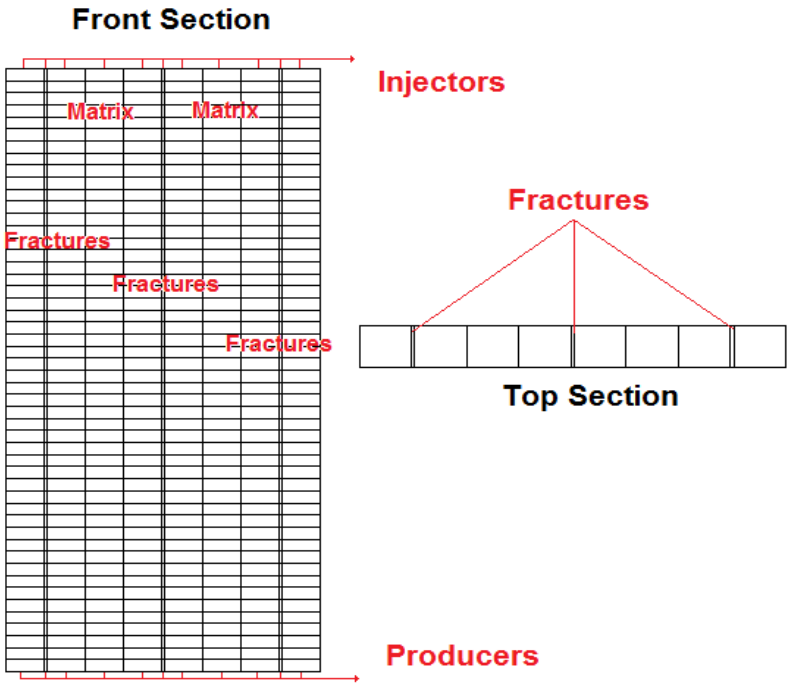

Figure 3-2: Base case grid models.

Table 3-1-1: Base case grid properties.

Direction	i	j	k
Number of Grid Blocks	11	1	50
Matrix Grid Block Dimensions, ft	0.5	0.5	0.2
Fracture Grid Block Dimensions, ft	0.033		

3.1.3. Rock Properties

The petro-physical properties of the rock are listed in Table 3-1-2. The model includes three discrete fractures that idealize the natural fractures system similar to those in the actual carbonate cores. The reservoir conditions are listed in Table 3-1-3. The relative permeability curves of the oil water and liquid gas used in the model are shown in Figures 3-3 and 3-4.

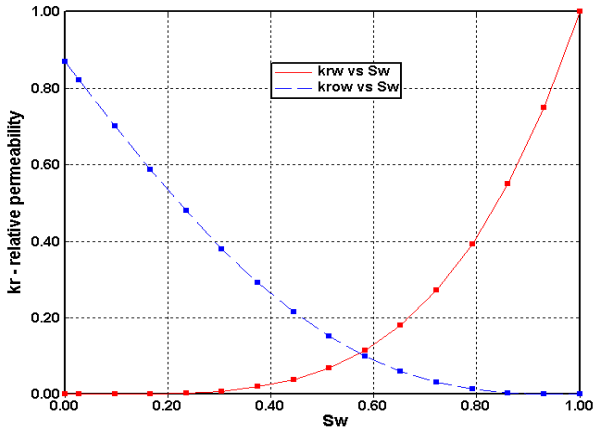

Figure 3-3: Water oil relative permeability curve.

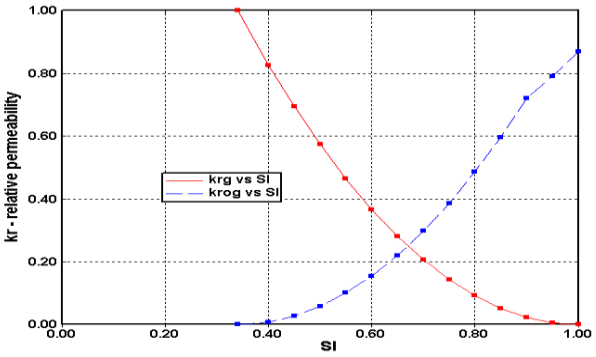

Figure 3-4: Gas liquid relative permeability curve.

Table 3-1-2: Base case rock properties.

Direction	i	j	k
Matrix Porosity	25%	25%	25%
Fracture Porosity	100%	100%	100%
Matrix Permeability	50 mD	50 mD	20 mD
Fracture Permeability	8000 mD		

Table 3-1-3: Base case reservoir conditions.

Initial Temperature, F	150
Initial Oil Saturation, %	72
Initial Water Saturation, %	28
Gravity Equilibrium	ON
Heat Loss	Off
Capillary Pressure Effect	On

3.1.4. Reservoir Fluids and Conditions

The model used in the simulator is a live, black-oil model with heavy, medium and light oil components. The oil compositions are given in Table 3-1-4. The production time is extended until the cumulative recovery curves stabilize that is 300 days.

Table 3-1-4: Oil composition.

Reservoir Fluids				
Properties	Heavy Oil	Medium Oil	Light Oil	Mixture
M.W, kg/kmol	600	450	250	493.17
Gravity, API	13.9	21.6	37.2	20.24
Mol. Fraction	0.97	0.02	0.01	1
Oil Viscosity at 150F, cp	1092	6.7	1.5	924
Volatility	Dead	Live	Live	

The reservoir injection conditions are summarized in Tables 3-1-5 and 3-1-6. The model assumes no heat loss and incorporates gravity equilibrium option and water-oil capillary pressure effect. It is to be mentioned that steam/gas injection temperature is lower than steam alone injection since the partial pressure of steam is reduced due to gas addition and, therefore, steam saturation temperature reduces as well.

Table 3-1-5: Base case steam injection conditions.

Steam Alone Injection	
Heat Loss	Off
Initial Temperature, F	150
Gravity Equilibrium	ON
Swi, %	28
So, %	72
Steam Injection Temperature, F	360
Steam Injection Pressure, psi	150
Steam Quality, %	90
Steam Production Pressure, psi	132

Table 3-1-6: Base case steam/gas injection conditions.

Steam/Gas Base Case	
Heat Loss	Off
Initial Temperature, F	150
Gravity Equilibrium	ON
Swi, %	28
So, %	72
Steam Injection Temperature, F	336.4
Steam Partial Pressure, psi	112.5
Total Injection Pressure, psi	150
Steam Quality, %	90
Steam Production Pressure, psi	132
Steam Molar Volume, %	75
Gas Molar Volume, %	25

3.1.5. Base Case Results

It is appropriate before introducing the parameter variations analysis to study the base case model and investigate the current cumulative recovery for each injection scheme. Starting with the cumulative recovery analysis, Figure 3-5 shows the cumulative recovery trends for steam, steam/N_2, and steam/CO_2 injections. The recoveries of the steam, steam/N_2, and steam/CO_2 are 43.98%, 44.21% and 42.92%, respectively. At early times, up to 21 days, both co-injected gases show better recovery than steam alone injection. This is shown in Figure 3-6. It can be seen from that figure that steam/CO_2 injection yields greater recovery than the other two processes but then it drops at later time to be

the lowest while steam/N_2 injection remains the highest. In order to understand the reason behind the recovery trends for the three processes, a study of the reservoir temperature, oil viscosity and gas saturation are discussed.

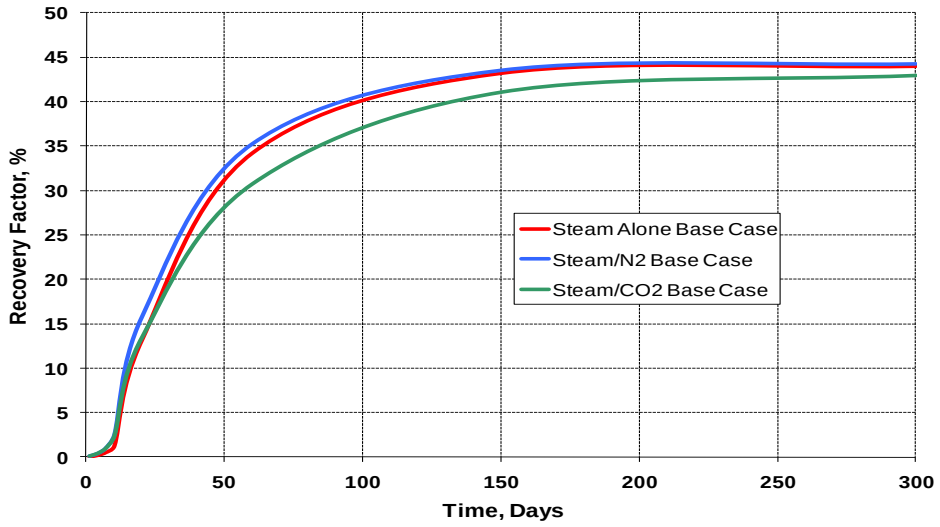

Figure 3-5: Base case cumulative recovery curve.

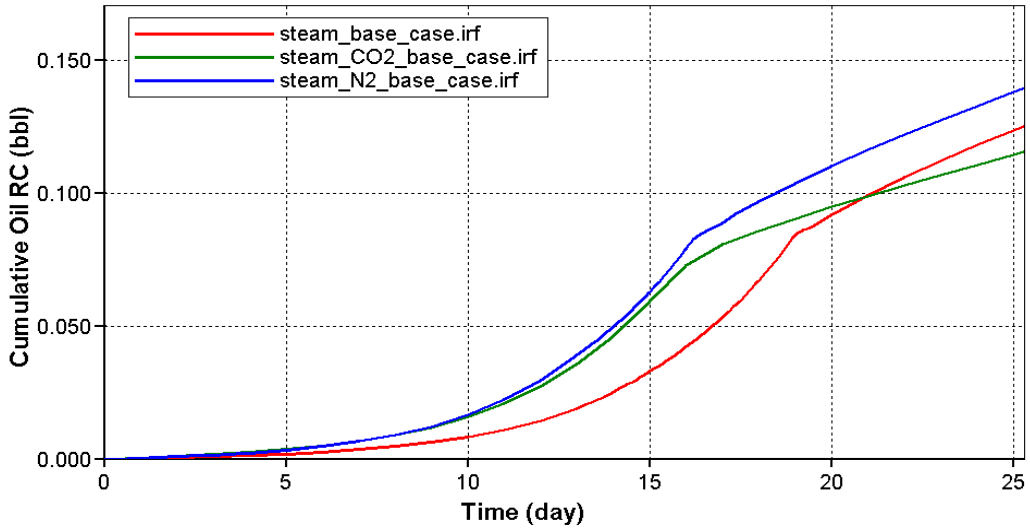

Figure 3-6: Base case cumulative recovery curve for 25 days.

Figure 3-7 presents the temperature profile for day 15 for the three schemes. In the steam/CO_2 process, the recovery was initially greater than steam alone process, meaning that the distribution of heat in the reservoir was more efficient in steam/CO_2 case at earlier time. The temperature profile, however, changed after 12 days of injection in that steam alone injection temperature distribution became better. This could mean that as the steam/CO_2 injection advances, CO_2 concentration keeps increasing in the reservoir blocking the steam from entering the reservoir. In the steam/N_2 case, the heat provided to the formation is the highest compared to steam and steam/CO_2. To explain this observation, it is indeed better to look at the gas concentration contour map to study the

reasons behind that but perhaps comparing the steam saturation is more convenient for the three processes in order to see how much heat is provided.

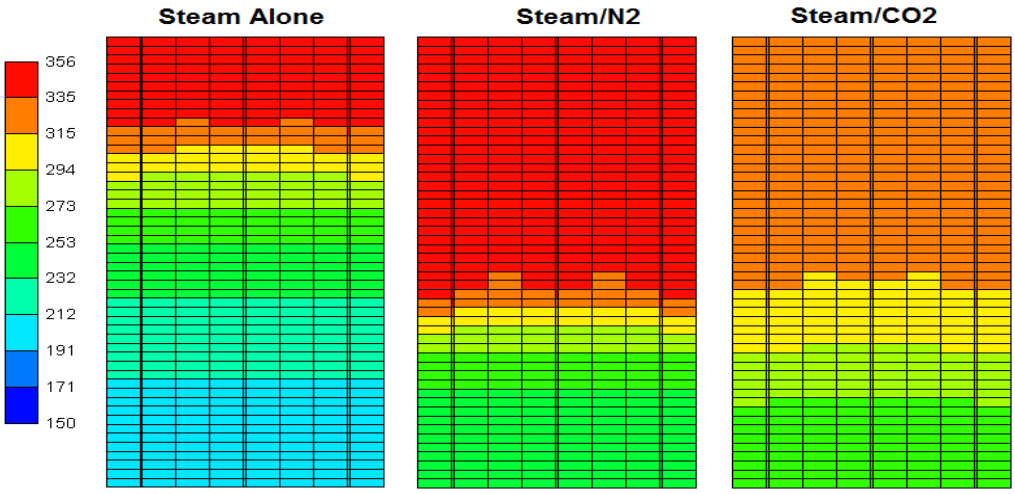

Figure 3-7: Base case temperature of profiles.

Figure 3-8 shows the steam Mole Fractions for the three floods at days 11, 12, 13 and 14 respectively. In the steam/CO_2 process it is clear that the steam concentration became less than in steam alone injection. This means that CO_2 mole fraction increased over 25%, that is the set concentration value, at some time during the production. This increase is due to the relatively small pressure drop across the system that led to block the steam mole fraction to some extent from entering the formation. Therefore, the volume of steam decreased in this case. This explains the lower temperature profile of co-injecting CO_2 and also the greater oil viscosity value obtained. Therefore, less oil drains after day 13 with steam/CO_2 process. As time proceeds, steam distribution becomes more stable and obtains the original concentration value of 75% while CO_2 concentration stabilizes at 25%. The fact that CO_2 was set to exist in the water and oil phases makes this process different from the steam/N_2 injection process.

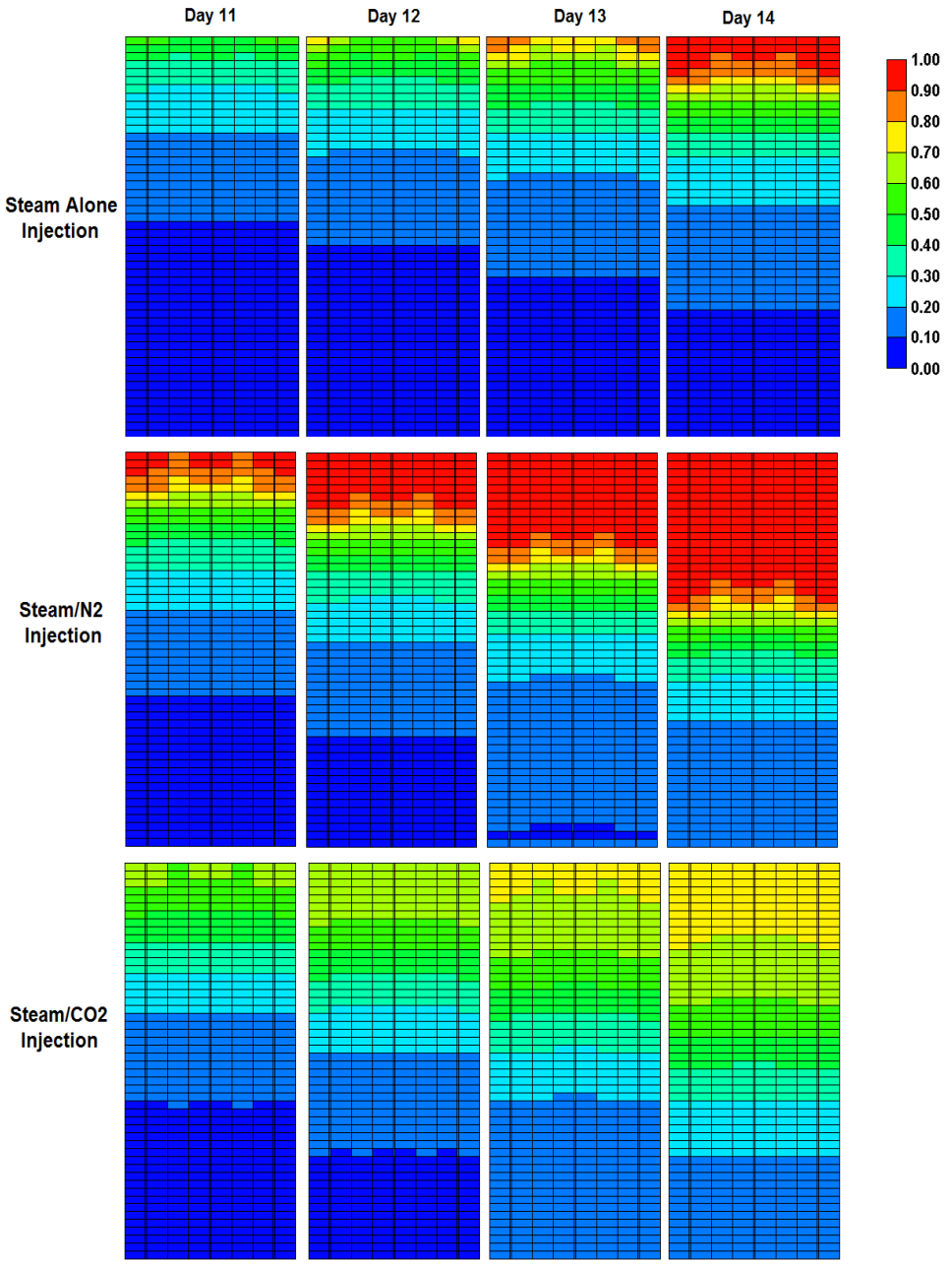

Figure 3-8: Base case steam mole fractions.

In the steam/N_2 injection case, however, the analysis is different. As mentioned previously, the amount of heat provided by steam/N_2 is greater than what was provided by steam alone. Figure 3-8 shows how greater steam concentration is during steam/N_2 injection compared to steam alone. This means that steam volume is larger in this case. To explain the reason behind this, Figure 3-9 shows the concentrations of N_2 and CO_2 in days 1, 2, 6, 10 and 16. It can be seen in the steam/N_2 case that N_2 concentration increases to almost 100% in the first day leaving very minimal concentration of steam in the formation. As time goes on, the steam concentration starts to increase gradually and it looks like steam is pushing nitrogen out of the formation. The addition of N_2 in the

steamflood process stabilizes the steam front propagation but not necessarily the gas front itself. At day 10, the steam/N_2 injection temperature exceeds the steam saturation temperature and the pressure starts to decrease indicating the increase in steam volume in the formation. The fact that steam front is more stable than the N_2 front and that N_2 does not exist in neither of oil nor water phases may explain why the gas concentration becomes close to zero at later time. When the gas concentration becomes very minimal, the process becomes more like steamflood process and the oil displacement efficiency drops to steam alone injection efficiency.

One of the main advantages of steam/gas injection is that the oil production starts earlier due to the early penetration of the gas into the formation. Even the steam itself when co-injected with the gas penetrates faster into the formation than steam alone injection. In the steam/CO_2 case, when the steam started to enter the formation and share it with the CO_2 the oil recovery became less since steam and CO_2 concentrations remained constant at 75% and 25% respectively. This may mean that only the gas existed in the formation prior to steam was the reason of improvements and not the co-existence of steam and gas. In the steam/N_2 case, nitrogen concentration reached almost zero at day 17 meaning that steam and N_2 did not co-existed in the reservoir but when the steam front became more stable it occupied the reservoir. This is why steam/N_2 injection still yielded greater recovery than steam/CO_2 injection. Steam alone injection works better than steam/CO_2 injection after the steam front becomes stable.

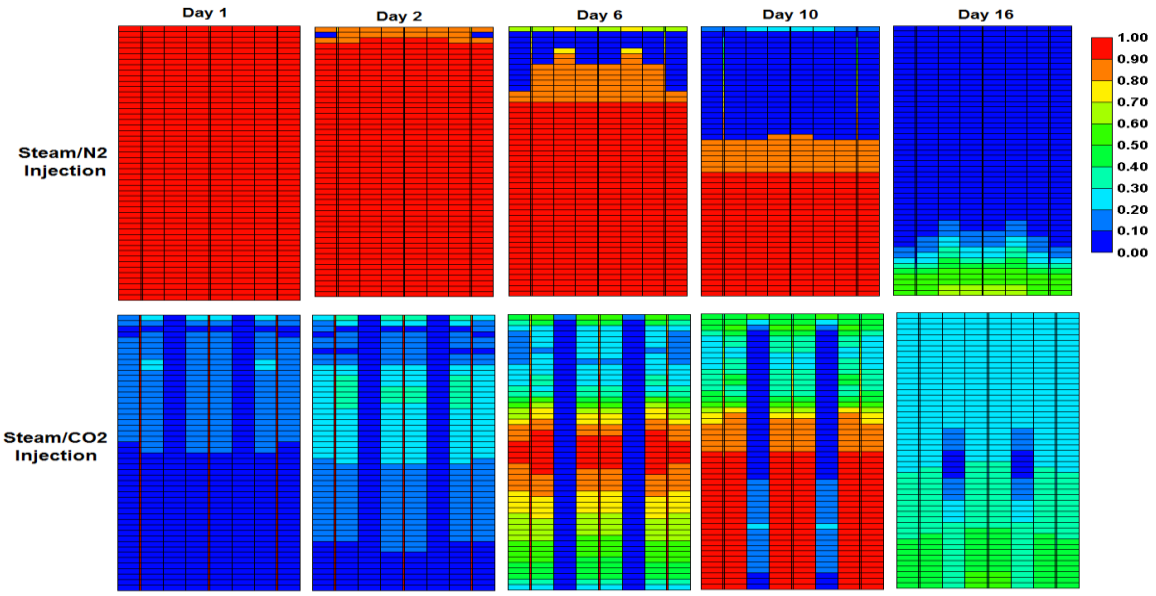

Figure 3-9: Base case N_2 and CO_2 concentrations.

Looking at the flow rate curves for the three processes, Figure 3-10, it can be seen that N_2 addition has accelerated the production flow rate and that breakthrough occurred earlier to steam alone flow rate. This observation has been confirmed by Hutchinson et al. (1983) and T.G. Harding et al. (1983). It can also be seen that steam/CO_2 broke through

before steam alone injection at lower rate. This can be explained by the temperature profile provided in Figure 3-7.

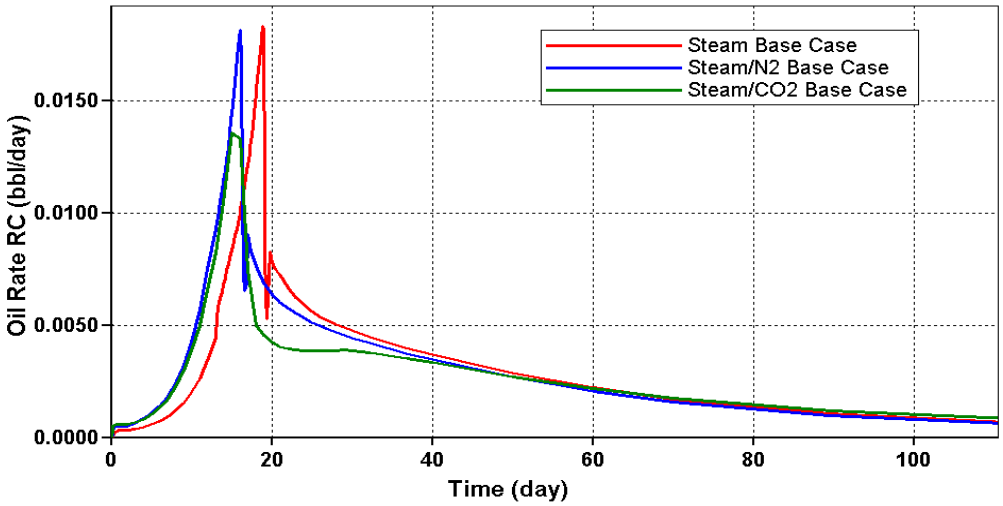

Figure 3-10: Base case production flow rate curves.

Steam/CO_2 flow rate starts to decrease after day 3 after being the highest. Zooming at the period of four days, Figure 3-11, shows that steam/CO_2 injection is advantageous over steam/N_2 injection for a certain period of time then the flow rate drops. This is because N_2 concentration in the reservoir reaches high levels at the first day of injection and then the levels start to decrease to very minimal values while CO_2 concentration at first day is so small. This means that the existence of the nitrogen at high concentrations decreases the steam volume and may lead to possible blockage of oil passage in the fractures due to the high mobility of the gas. At later time, however, the N_2 concentrations become very small while steam dominates in the pores and pore throats. This explains the increase in the production flow rate after day 3. On the other hand, CO_2 concentrations remain at 25% and, therefore, the flow rate drops.

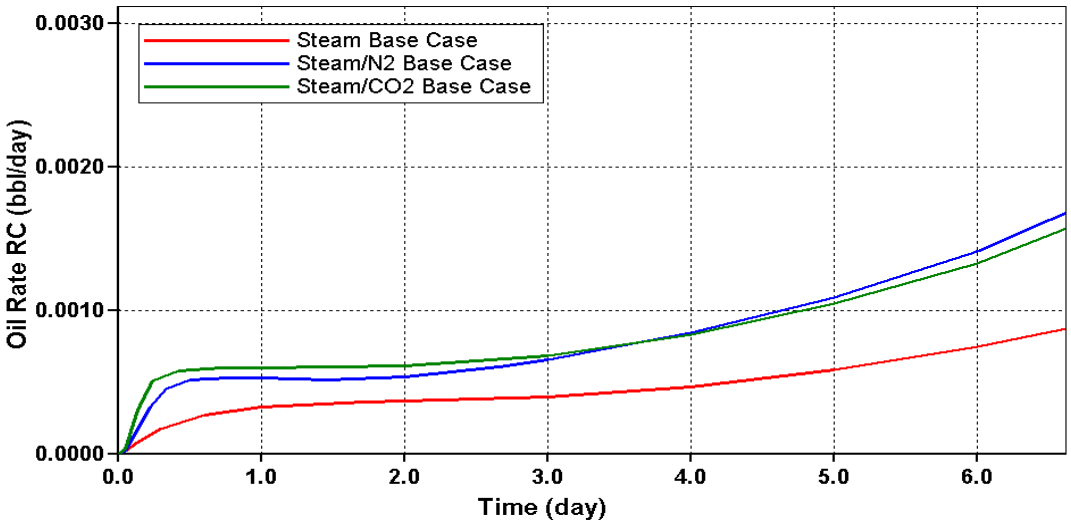

Figure 3-11: Base case zoomed production flow rate curve.

This raise two observations, first, steam/CO_2 broke through slightly earlier than steam alone injection. Therefore, the early breakthrough is a property of the added gas whether it was condensable or non-condensable but with non-condensable the breakthrough is clearly earlier than steam injection. Second, the condensable gas co-injection yields lower flow rate and recover less oil.

3.2. Parameters Analysis

3.2.1. Oil Gravity

Three different oil gravities are studied in this section. The oil gravity values to be studied are 14 API, 28 API and 37 API where the base case oil gravity is 14API. The objective of this study is to investigate the effect of co-injecting gas on the recovery of heavy, medium and light oil types.

It was noticed that the trends obtained from plotting the cumulative oil recovered for the three gravities for each injection scheme are very similar. Therefore, explaining one scheme should illustrate the effects on the different gravities. Figure 3-12 shows the recovery curve of steam/CO_2 injection. It can be seen that as the oil gravity increases the recovery increases as well. There are many factors that control these trends. For example, as the viscosity of oil decreases the gravity number increases meaning that the oil is more influenced by gravity. This is exactly what is happening at early time of production in that sharper production recoveries and flow rates are obtained as the oil gravity increases. This can be noticed in the flow rate curves in Figure 3-13. At lower oil viscosities, the steam and the gas penetrate the formation faster than at greater oil viscosities leading to earlier heating and pushing drive to the oil as well as breakthrough. Figure 3-14 shows the CO_2 concentrations at different gravities. As a result, the injection profile becomes more stable for greater gravities as shown in the figure. This includes steam alone and steam/N_2 injections as well in that steam penetrates faster in the formation for greater gravities and so the N_2. Therefore, the co-injection of gases improves the steam injectivity.

Another point to mention is the attitude of CO_2 in lighter oil types. When dealing with CO_2 as a condensable gas, the solubility of the gas decreases in the oil as the temperature increases. In fact, according to Bader et al (1979) and Jacobs et al (1980) the effect of gas in solution on reducing the oil viscosity decreases as the temperature increases above 100^oC. Therefore, the recovery is relatively less improved by the addition of gases for oil with greater gravities. The effect of adding N_2 on lighter oil gravities is represented in supporting the driving pressure and providing the extra heating brought by the increase in steam volume resulted from steam partial pressure reduction.

Nevertheless, one problem with the presented results is that for the three different gravities, the water-oil capillary pressures were the same that may not be accurate description. Therefore, there might be some inaccuracy in the medium and light oil gravity but the trends illustrate the general behavior.

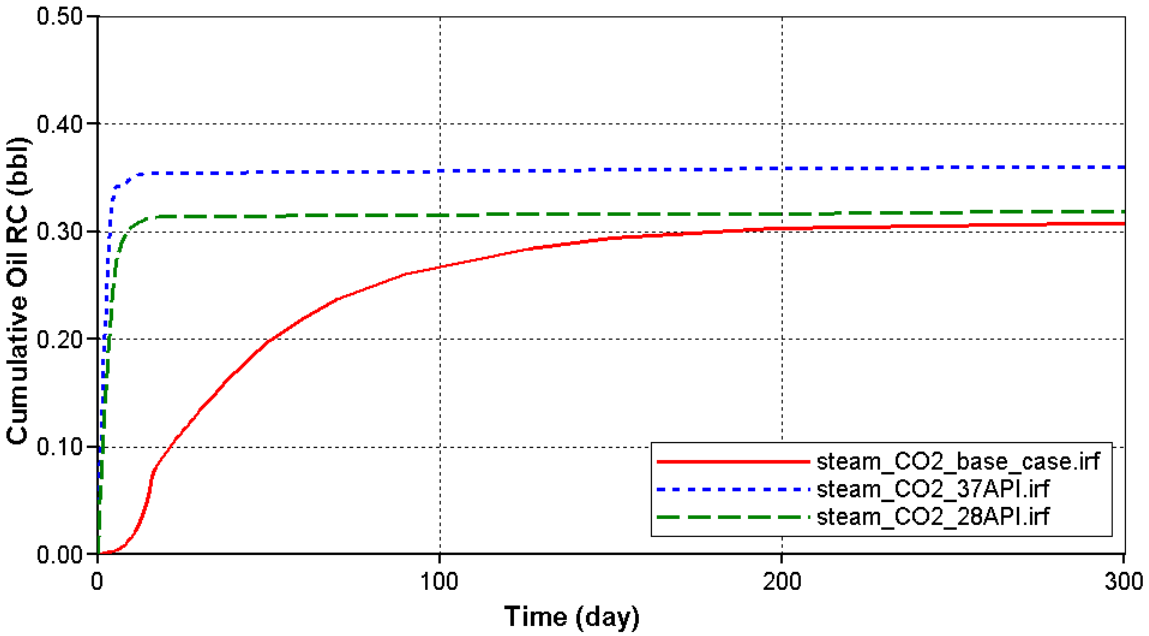

Figure 3-12: Oil gravity-steam/CO_2 recovery curves.

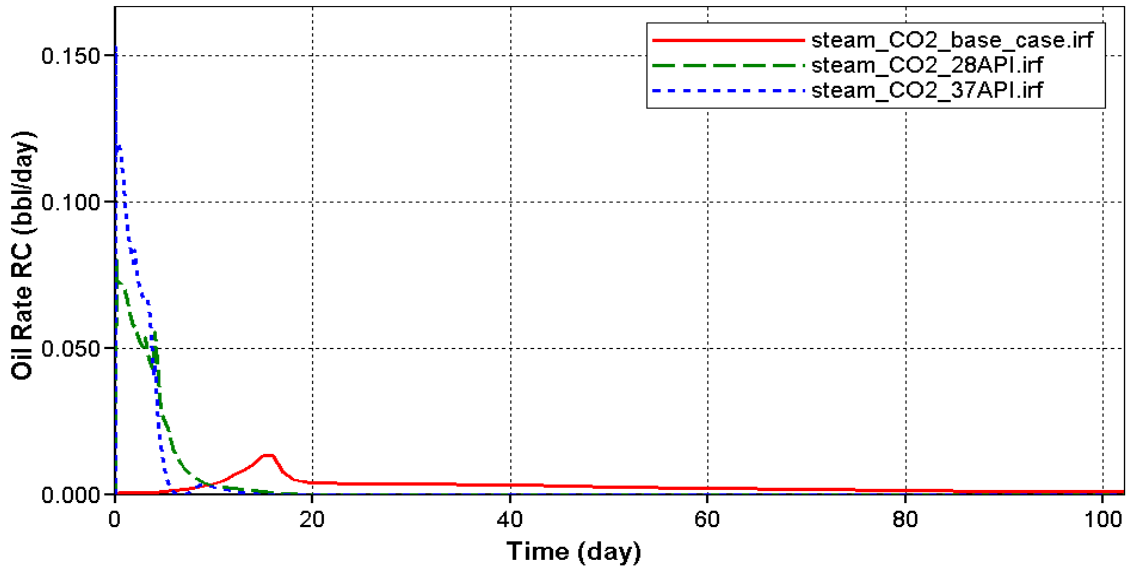

Figure 3-13: Oil gravity-steam/CO_2 flow rate curves.

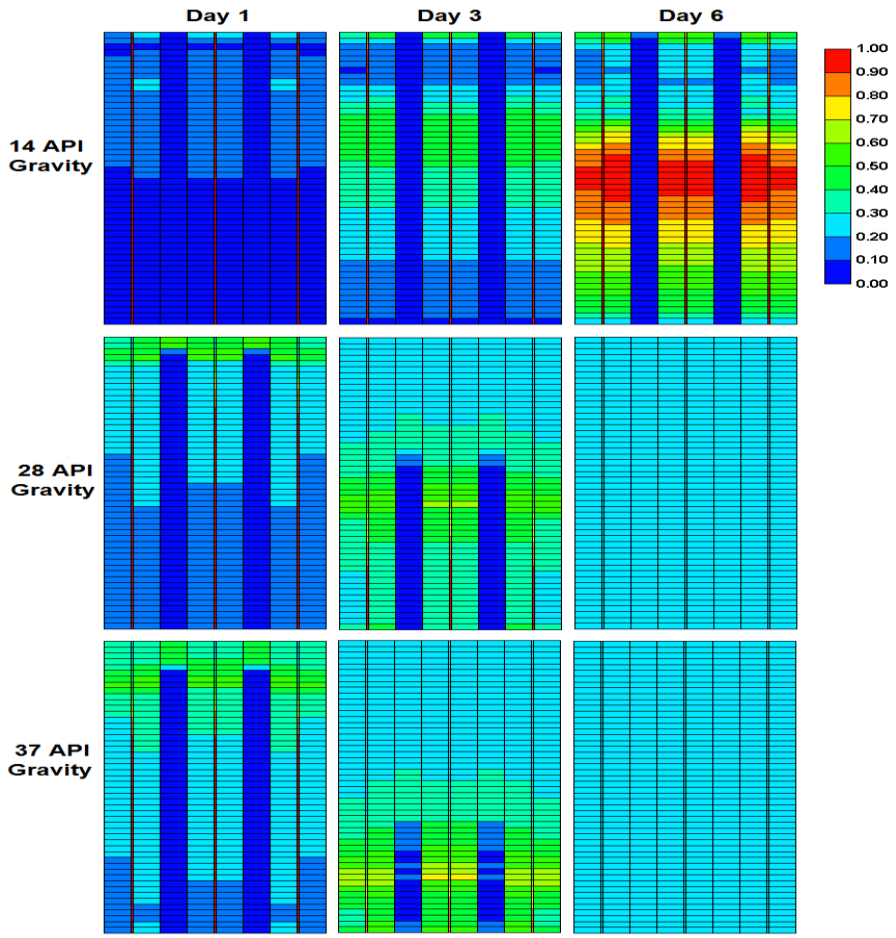

Figure 3-14: Oil gravity-CO_2 concentrations at different gravities.

3.2.2. Gas Concentration

This section discusses the effect of varying the concentrations of the co-injected gases on the base case oil recovery. The base case gas mole fraction is 25%. The study includes 10% and 40% mole fractions for both steam/N_2 and steam/CO_2. The change in the mole fractions affects the steam partial pressure and hence the steam temperature. The total injection pressure is the same for all the scenarios but steam partial pressure and temperature decrease as the gas concentration increases.

In the steam/CO_2 case, Figure 3-15 shows the cumulative oil curves for different CO_2 mole fractions. It can be seen that with mole fraction of 0.1 the recovery is the highest. The recovery decreases as the concentrations increase. Therefore, the greater the CO_2 concentration, the less the recovery is. This is because as the CO_2 concentration increases in the formation the volume occupied by the gas increases as well that reduces the amount of steam injected. In addition, the greater the concentration of the injected gas the more probable that steam would channel to the production wells. Therefore, the oil recovery decreases as the concentration of CO_2 increases due to reductions in steam injectivity. Another point to mention is that at early times the difference in recoveries of

the three concentrations is insignificant. This may indicate that gravity drainage is perhaps the main producing mechanism for that period of time.

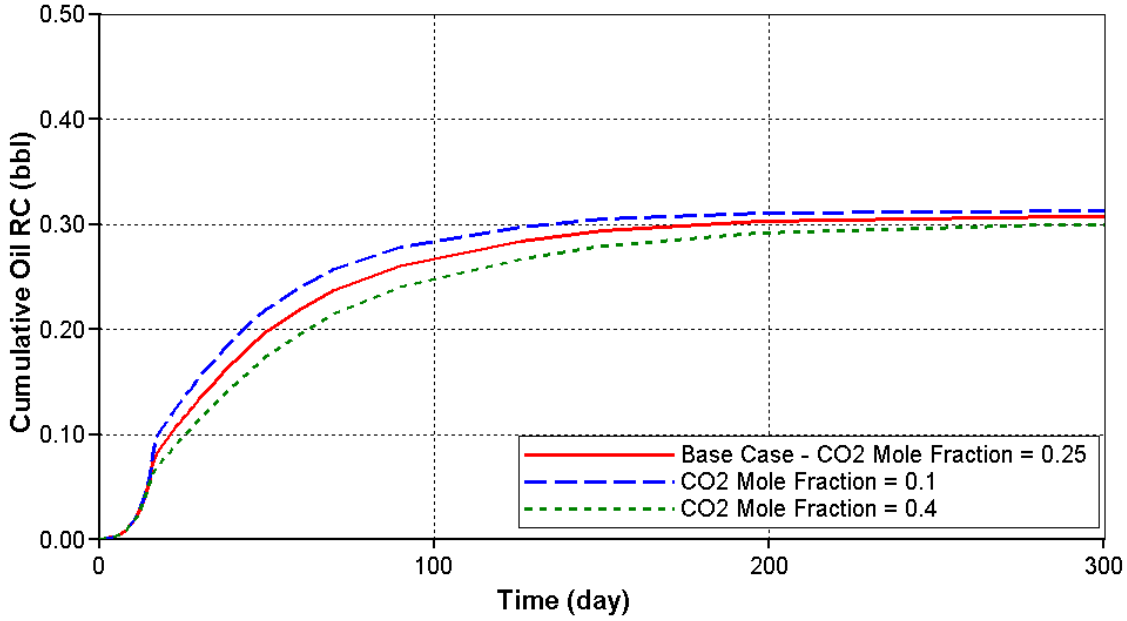

Figure 3-15: Gas concentration-cumulative oil recovery curves for CO_2 concentrations.

The steam/N_2 case is different as represented by the recovery curves in Figure 3-16. There is no pronounced difference between the three concentrations. The reason behind that is better explained by the gas concentration contour map in Figure 3-17.

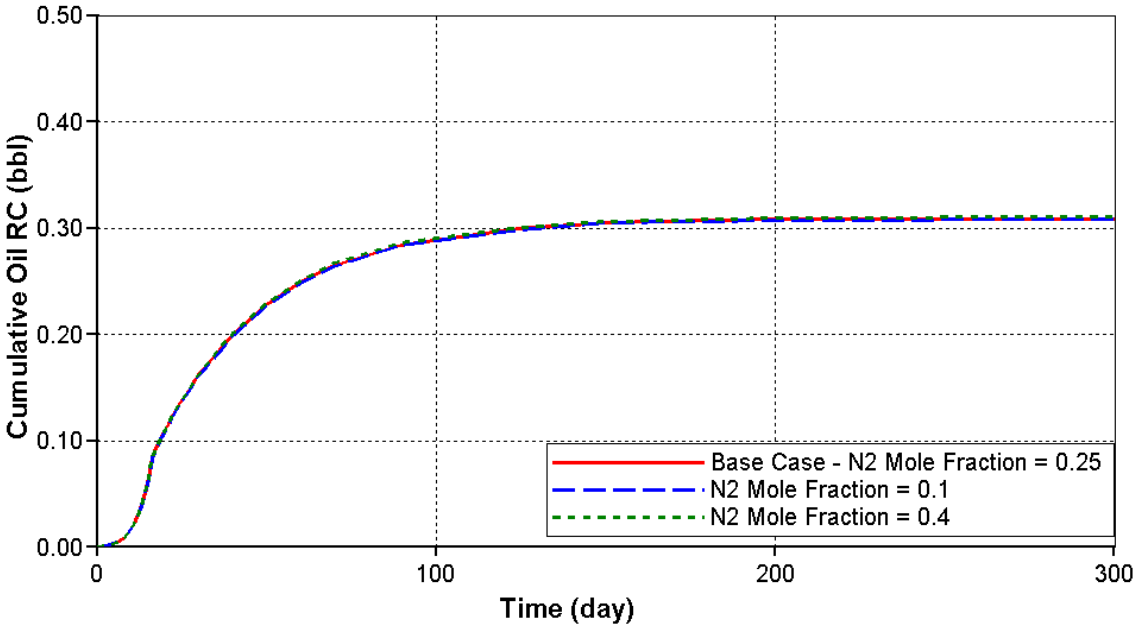

Figure 3-16: Gas concentration-cumulative oil recovery curves for N_2 concentrations.

Figure 3-17 shows the N_2 concentrations profiles for the studied values at days 3, 7 and 14. The figure shows that in day 3 the mole fraction of N_2 is the same for all the cases. The same observation is noticed for days 7 and 14. This means that no matter how much the injected fluid contain N_2 it will eventually reach very minimal value of less than 1% for the reasons mentioned previously.

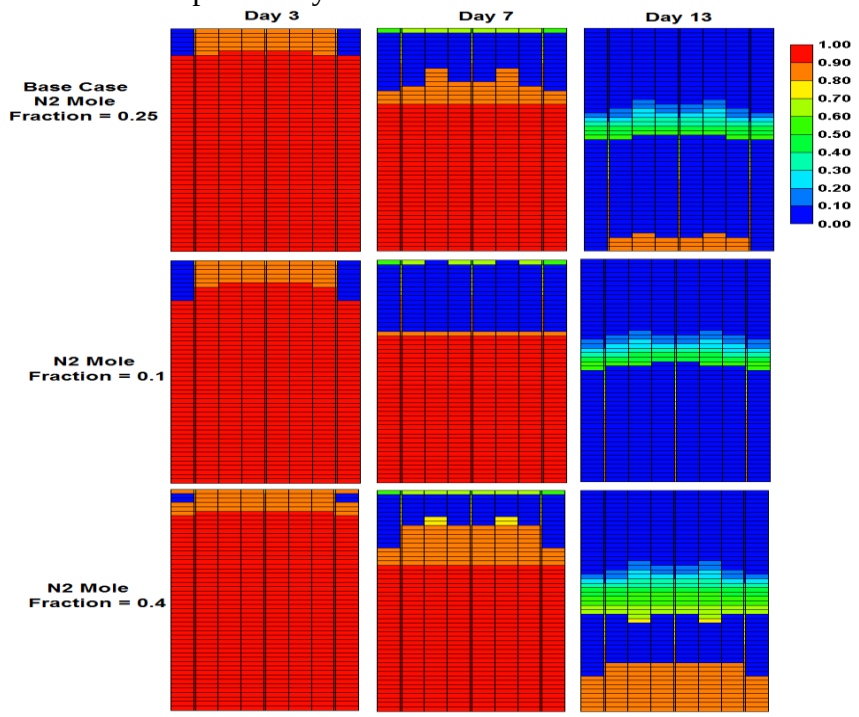

Figure 3-17: Gas concentration-N_2 mole fraction map during days 3, 7 and 14

3.2.3. Effects of Steam Temperature and Partial Pressure during Steam/Gas Injection

The purpose of exploring the effects of steam temperature and partial pressure is to gain an understanding of how the interplay of temperatures and pressures affect the role of the co-injected gases and hence affect the oil recovery. In the steam alone injection, the steam temperature, 360^{o}F, corresponds to the steam saturation pressure. The cases introduced in the analysis are shown in Table 3-2-1. The first case is the base case of steam/gas injection. The second case is increasing the steam injection temperature to the original value of steam alone injection. The third case is basically increasing the temperature further above the saturation temperature.

Table 3-2-1: Steam temperature and partial pressure values.

Case	Steam Temperature, F	Steam Partial Pressure, psi	Total Injection Pressure, psi
1- (Base Case)	337	112	150
2	360	150	150
3	400	150	150

The cumulative recovery curve in the steam/CO_2 case shown in Figure 3-18 shows no significant difference in recovery between the three cases but it gives some enlightenments. First, the responsible heat of reducing the oil viscosity is the steam latent heat of vaporization and, therefore, superheating the steam has little effect on recovery. When increasing the steam temperature from case 1 to case 2 it is noticed that the recovery curve slightly drops. The same occurs to case 3 in that the recovery curve drops further. The extra heat provided by the greater temperatures does not contribute in heating the reservoir as long as the gas concentration stays constant. This explains why the temperature never exceeds 332F that is the steam saturation temperature in the temperature contour map in the simulation. Regarding the decrease in the recovery curves, it may be due to the reduction in CO_2 solubility in the oil as the temperature increases.

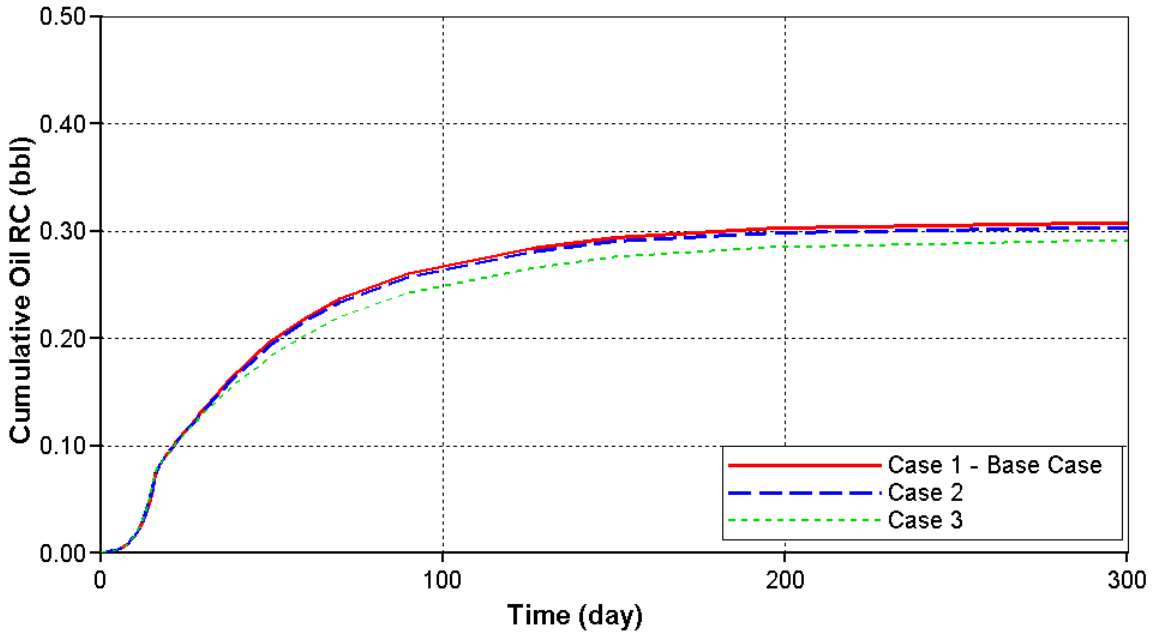

Figure 3-18: Steam temperature-steam/CO_2 cumulative recovery curve for different steam temperatures.

In the steam/N_2 case, as shown in Figure 3-19, the oil recovery is the same for the three cases. This may be because of the insolubility of N_2 that makes temperature variations ineffective in affecting the gas role in recovery. The extra heat provided in cases 2 and 3 does not increase the formation temperature and, therefore, the oil viscosity stays almost the same.

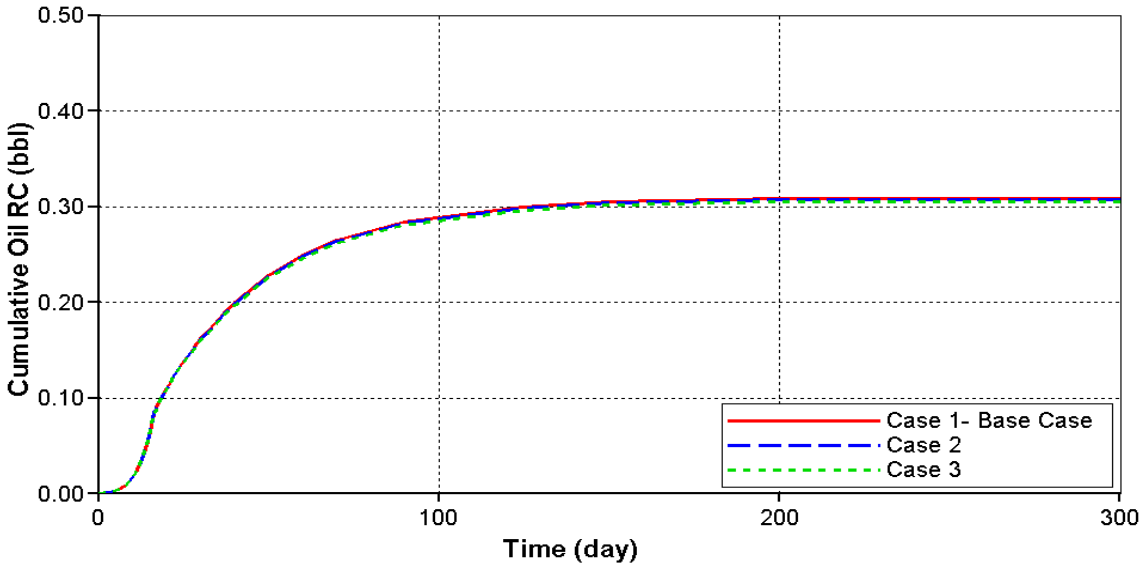

Figure 3-19: Steam temperature-steam/N_2 cumulative recovery curves for different steam temperatures.

Result

Chapter 4

4. Numerical Modeling

4.1. Prototype and Original Models Description

The prototype experiment consists of a short core with a length of 3.5 inches while the original experiment core has a length of 28 inches as mentioned in the numerical analysis description section. The following paragraphs present briefly the two models properties used in the simulation work.

4.1.1. Oil Viscosity

The oil used in the study has a gravity of 14 API with viscous nature. It is the same oil type as the one used in the base case study. The oil properties and the viscosity-temperature plot are found in Table 3-1-4 and Figure 3-1 respectively, in the sensitivity analysis section. The oil viscosity at a temperature of 150^0 F, the reservoir temperature, is about 945cp.

4.1.2. Grid System

The gridding system used in the prototype and original experiments is 2-D Cartesian model with gravity drainage option and capillary pressure effects. The grid system is similar to the one used in the sensitivity analysis except that the numbers and dimensions of the grids are different in addition to the permeability and porosity values. The reservoir model is shown in Figure 4-1. The Grid properties for both experiments are found in Table 4-1-1.

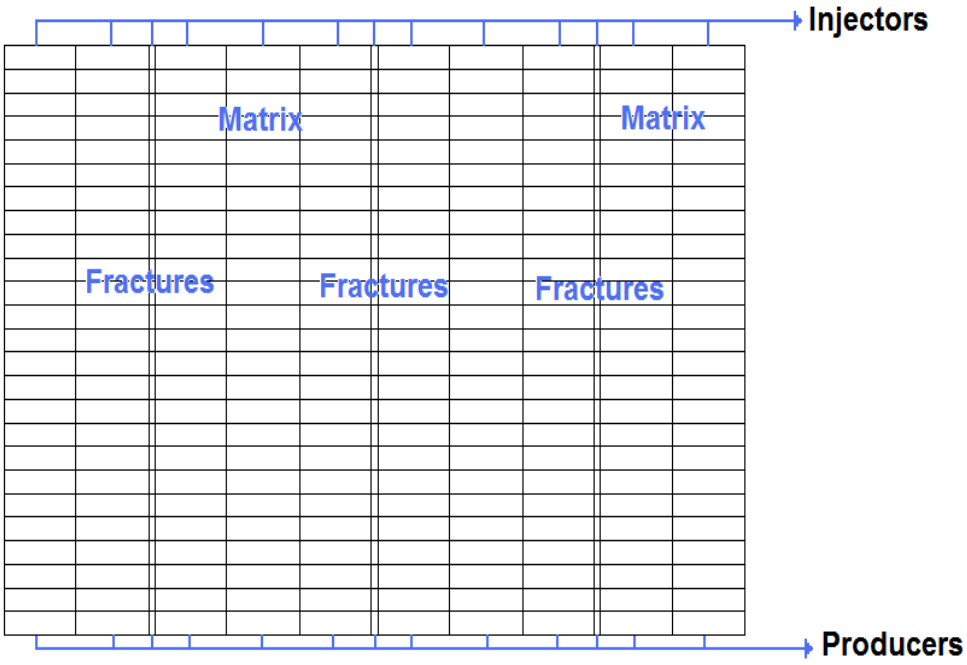

Figure 4-1: Prototype and original grid models.

Table 4-1-1: Prototype and original grid properties.

Experiment	Prototype			Original		
Direction	i	j	k	i	j	k
Number of Grid Blocks	13	1	25	13	1	102
Matrix Grid Block Dimensions, ft	0.0347	0.0347	0.0116	0.0358	0.0358	0.0225
Fracture Grid Block Dimensions, ft	0.002891667			0.002983		

4.1.3. Rock Properties

The two models use heterogeneous petro-physical properties. The average permeability and porosity values of both experiments are 0.5 mD and 9.4% respectively. Table 4-1-2 lists the rock properties. The relative permeability curves of the oil-water and liquid-gas are the same as the one used in the sensitivity analysis section, Figure 3-3 and Figure 3-4.

Table 4-1-2: Prototype and original rock Properties.

Direction	i	j	k
Matrix Porosity	9.4%		
Fracture Porosity	100%		
Matrix Permeability	2.5 mD	2.5 mD	0.5 mD
Fracture Permeability	1000 mD		

4.1.4. Reservoir Fluids

The model used in the simulator is a live, black oil model with heavy, medium and light oil components. The oil compositions are given in Table 3-1-4. The reservoir injection conditions for the prototype and original experiments are summarized in Tables 4-1-5, 4-1-6, 4-1-7 & 4-1-8.

Table 4-1-5: Prototype steam injection conditions.

Prototype Experiment	
Steam Alone Injection	
Heat Loss	Off
Initial Temperature, F	150
Gravity Equilibrium	ON
Swi, %	28
So, %	72
Steam Injection Temperature, F	348
Steam Injection Pressure, psi	129
Steam Quality, %	90
Steam Production Pressure, psi	127

Table 4-1-6: Prototype steam/gas injection conditions.

Prototype Experiment	
Steam/Gas Base Case	
Heat Loss	Off
Initial Temperature, F	150
Gravity Equilibrium	ON
Swi, %	28
So, %	72
Steam Injection Temperature, F	327
Steam Partial Pressure, psi	96.75
Total Injection Pressure, psi	129
Steam Quality, %	90
Steam Production Pressure, psi	127
Steam Molar Volume, %	75
Gas Molar Volume, %	25

Table 4-1-7: Original steam injection conditions.

Original Experiment	
Steam Alone Injection	
Heat Loss	Off
Initial Temperature, F	150
Gravity Equilibrium	ON
Swi, %	28
So, %	72
Steam Injection Temperature, F	360
Steam Injection Pressure, psi	143.58
Steam Quality, %	90
Steam Production Pressure, psi	127

Table 4-1-8: Original steam/gas injection conditions.

Original Experiment	
Steam/Gas Base Case	
Heat Loss	Off
Initial Temperature, F	150
Gravity Equilibrium	ON
Swi, %	28
So, %	72
Steam Injection Temperature, F	334
Steam Partial Pressure, psi	107.68
Total Injection Pressure, psi	143.58
Steam Quality, %	90
Steam Production Pressure, psi	127
Steam Molar Volume, %	75
Gas Molar Volume, %	25

4.2. Prototype Experiment Results and Discussion

The simulation of the prototype experiment yielded a similar trend to what was presented in the sensitivity analysis. Figure 4-2 shows the cumulative oil recovered over a period of 50 days. The steam/gas co-injections show a clear advance in terms of recovery at early time compared to steam alone injection. Both N_2 and CO_2 show similar effect at the first

day but then the nitrogen contributes better toward the recovery. This is attributed to the gas invasion during the injection and is discussed after the next paragraph.

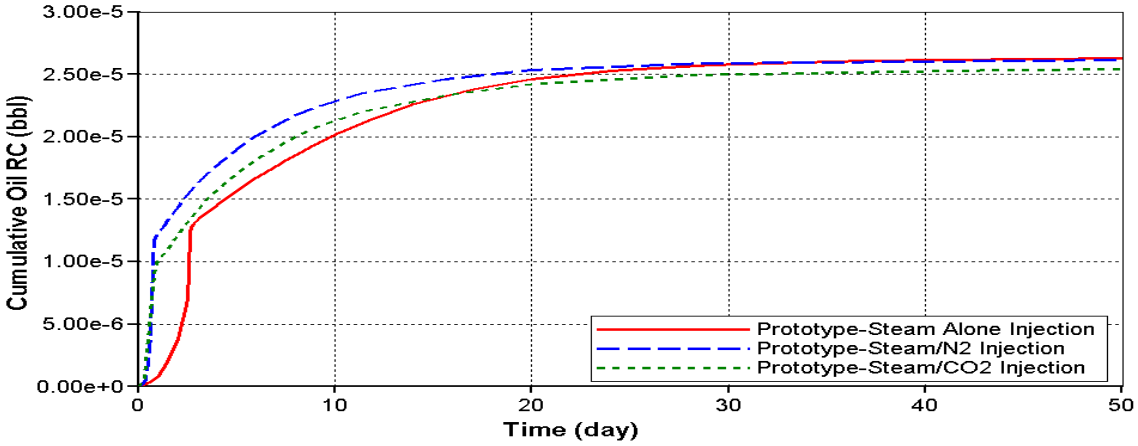

Figure 4-2: Prototype-cumulative oil recovery curves.

Another way of representing the recovery is by introducing the recovery factor curves vs. pore volume injected of steam in CWE, Figure 4-3. The curves show that the recovery factors of steam, steam/N_2 and steam/CO_2 processes are 45.58 %, 45.22 % and 42.87 % respectively. The curves also tell that steam/CO_2 injection required the largest injection volume of water in comparison with steam and steam/N_2 injections.

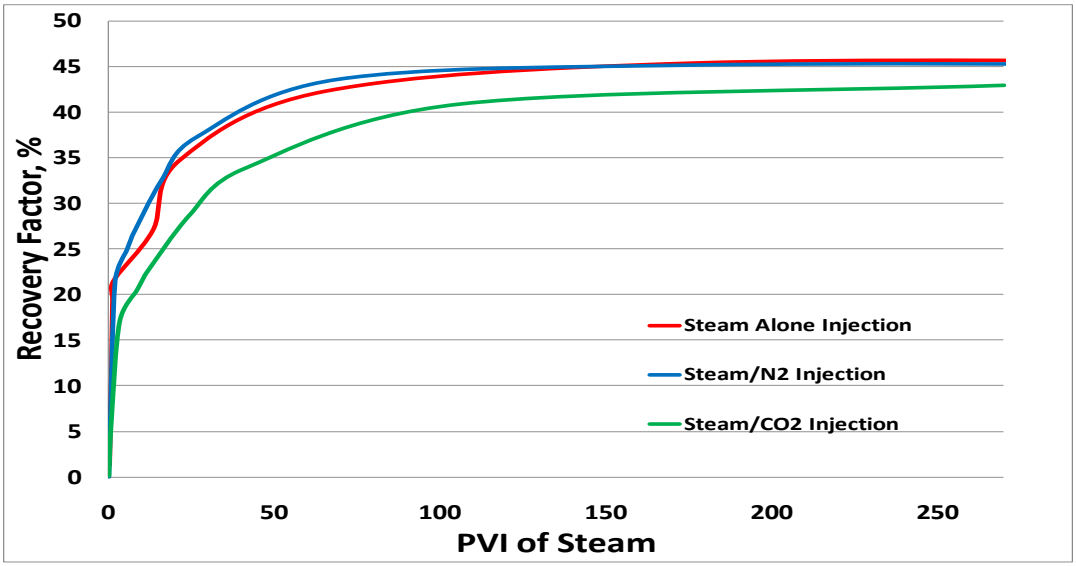

Figure 4-3: Prototype-recovery versus PVI of steam curves.

In order to examine the decrease in recovery by steam/CO_2 process in later times, the mole fractions of steam for the three processes are studied and presented in Figure 4-4. It can be noticed that in the steam alone case, the steam enters the formation at later time while in the case of gas co-injections the steam entered earlier to the formation. The co-injected gases increased the volume of steam injected by reducing steam partial pressure. Therefore, steam was more efficient in the gas co-injection cases and the recovery increased steeply at early times unlike steam alone case that showed gradual rise.

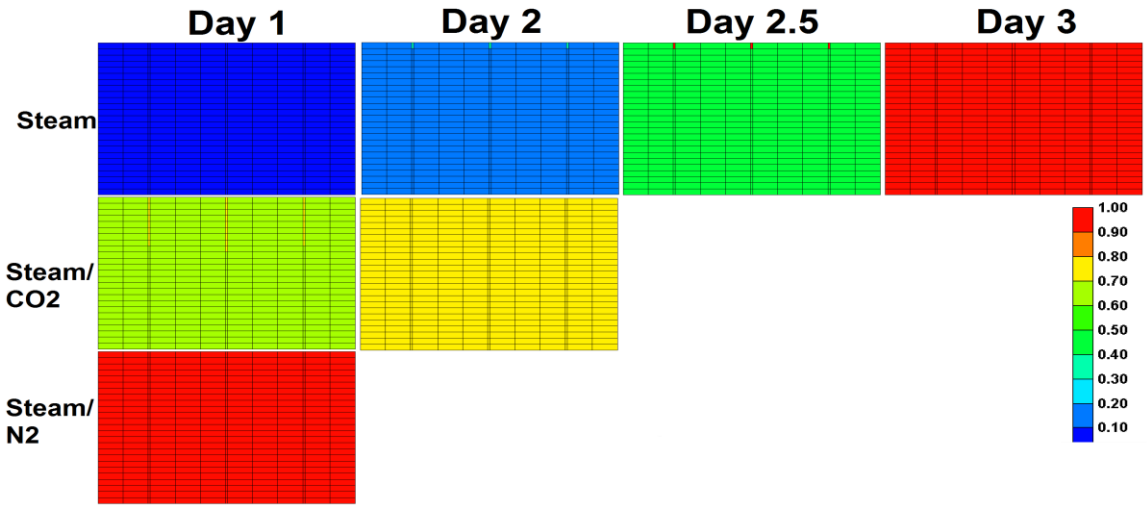

Figure 4-4: Prototype-steam mole fractions for the three processes.

The temperature maps are no different. Figure 4-5 shows that in the steam alone injection the temperature of the formation increases later than in the gas co-injection cases. The difference between the temperature profile of steam alone injection in day 3 and steam/CO_2 in day 1 is about 30^{o}F. In steam/N_2 injection case the temperature at day 1 is equal to the temperature of steam alone case at day 3. The difference in time is the main source of the additional recovery obtained by the gas co-injection cases at the early time of production.

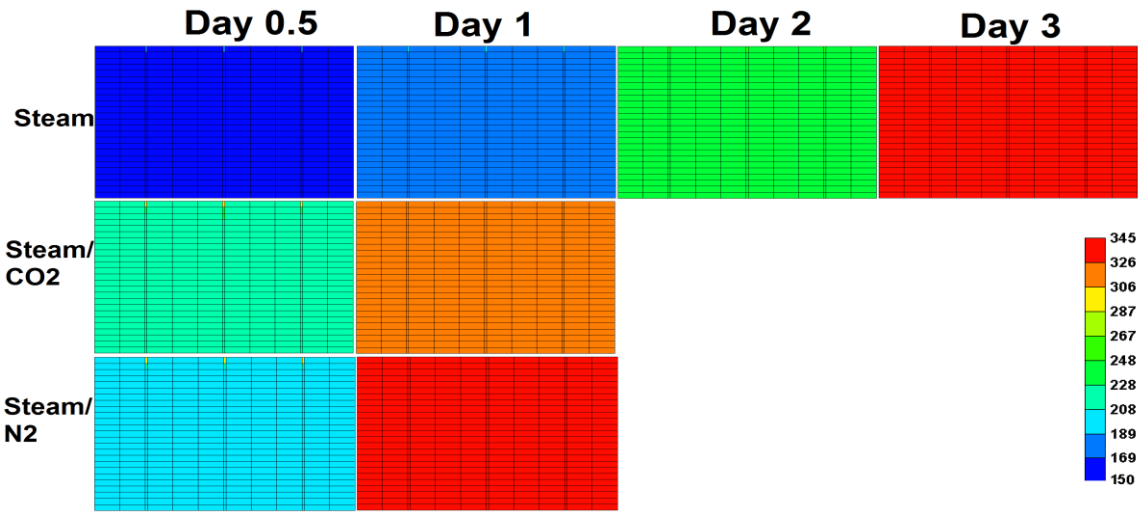

Figure 4-5: Prototype-formation temperature.

Looking at the flow rates of the three cases, Figure 4-6 it is clearly observed the flow rate accelerations resulted from the addition of the gases into the steamflood process. Breakthrough occurs very fast in the steam/N_2 and steam/CO_2 cases when compared to steam alone. This is perhaps another reason why the production recoveries of the steam/gas injections decrease at later time. Nevertheless, this is a beneficial for production especially for short-term production operation.

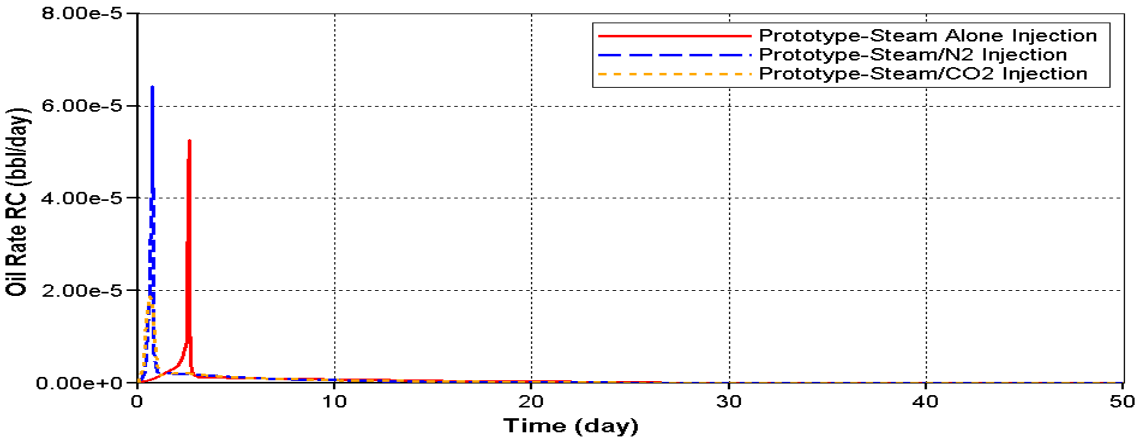

Figure 4-6: Prototype-oil flow rates.

4.3. Original Experiment Results and Discussion

The simulation of the long core experiment, original, showed similar trends of the results. Therefore, the recovery curves, Figure 4-7, were similar to the prototype experiment in behavior. There are, however, two observations that were noticed in the long core results that are discussed in the comparison section next. Figure 4-8 shows the recovery factors of the three processes that are 45.49%, 45.71% and 43.28% for steam, steam/N_2 and steam/CO_2 respectively. The flow rate curves, Figure 4-9, show flow rates acceleration for steam/gas injection over steam alone injection and the spikes indicate breakthrough points.

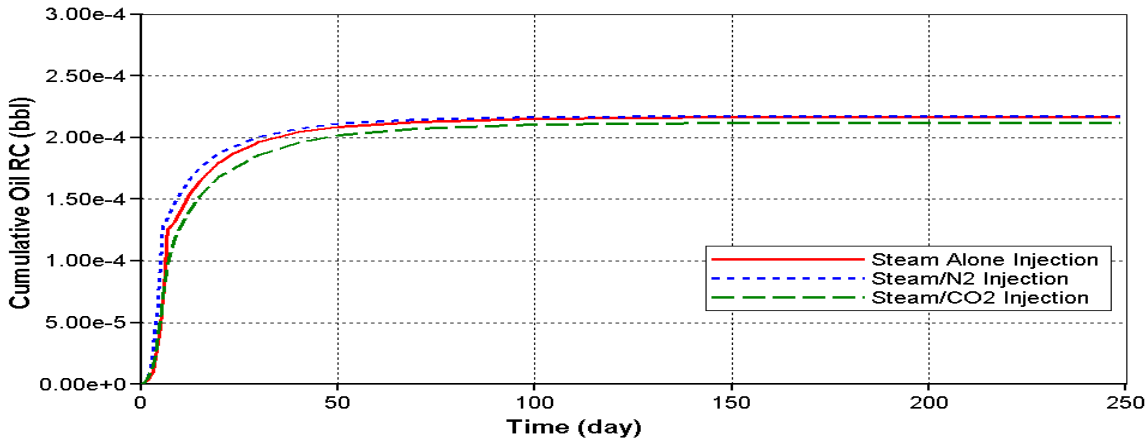

Figure 4-7: Original-cumulative recovery curves.

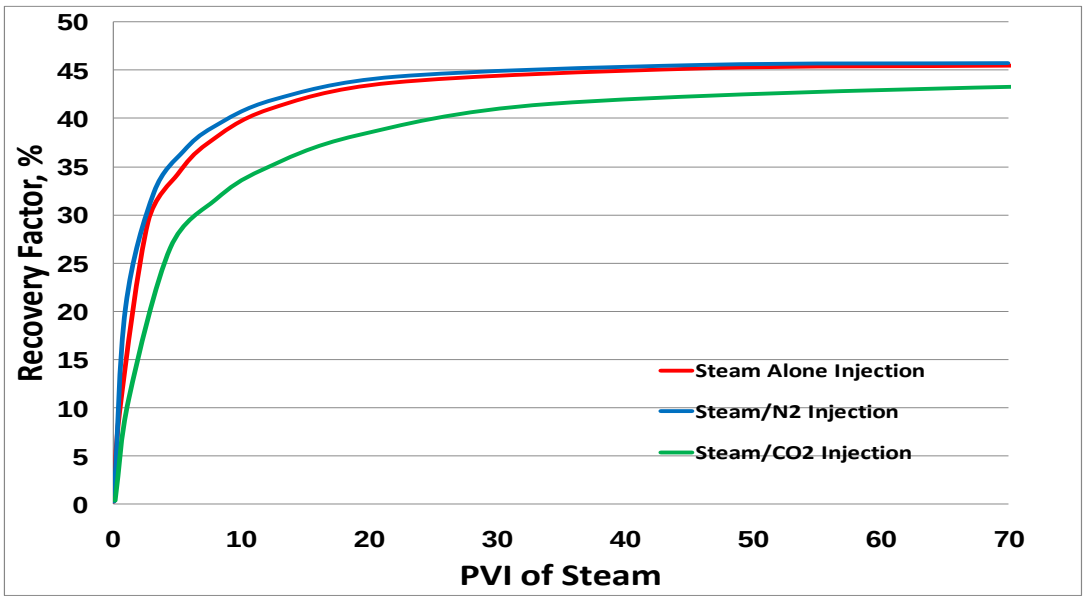

Figure 4-8: Original-recovery factor curves.

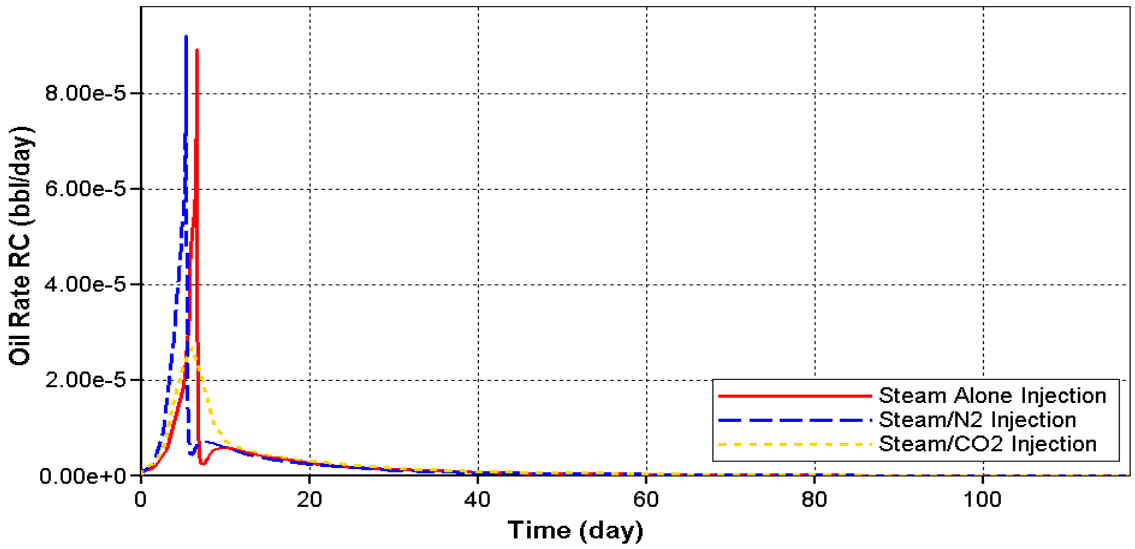

Figure 4-9: Original flow rate curves.

4.4. Prototype and Original Results Comparison

Comparison of the results obtained from the prototype and original experiments are necessary. This is to demonstrate the benefits provided by the gravity effect on oil recovery when injecting the fluids simultaneously. Gravity drainage is a proven mechanism in that heavy-oil is produced by. In general, the strength of gravity depends on mass and distance. If the core exceeds a certain length of height, then it is said that the gravity force domination is greater than the rock capillarity. Such a discussion usually requires calculations of bond and capillary numbers to confirm the multiphase flowing regime in pores network. Nevertheless, in these experiments the pressure drop was set to be the same, 0.57 psi/inch. In addition, the averaged porosity and permeability values

were the same. The relative permeability curves and the capillary pressure values are all the same. The injection and production conditions are the same. This is to hold all the parameters constant and observe the effect of length, i.e. gravity, on oil recovery. The following paragraphs compare the results of each process from the two experiments.

Comparing the steam alone injection process, Figure 4-10 shows the recovery factor of the prototype and original experiments for given pore volume injected. The original experiment recovery curve is greater at most of the time than the prototype curve. This indicates the acceleration in oil production generated by the effect of gravity on production rate. The gravity effect, therefore, contributed to additional recovery for greater PVI values. Both experiments yielded the same ultimate recovery value and this is expected due to the similarity in the pressure gradient value and the similar rocks and fluids properties. The same conclusion can be said about the steam/N_2 and steam/CO_2 processes in which the recovery was accelerated in the original experiment and yielded greater volumes for longer period of injections.

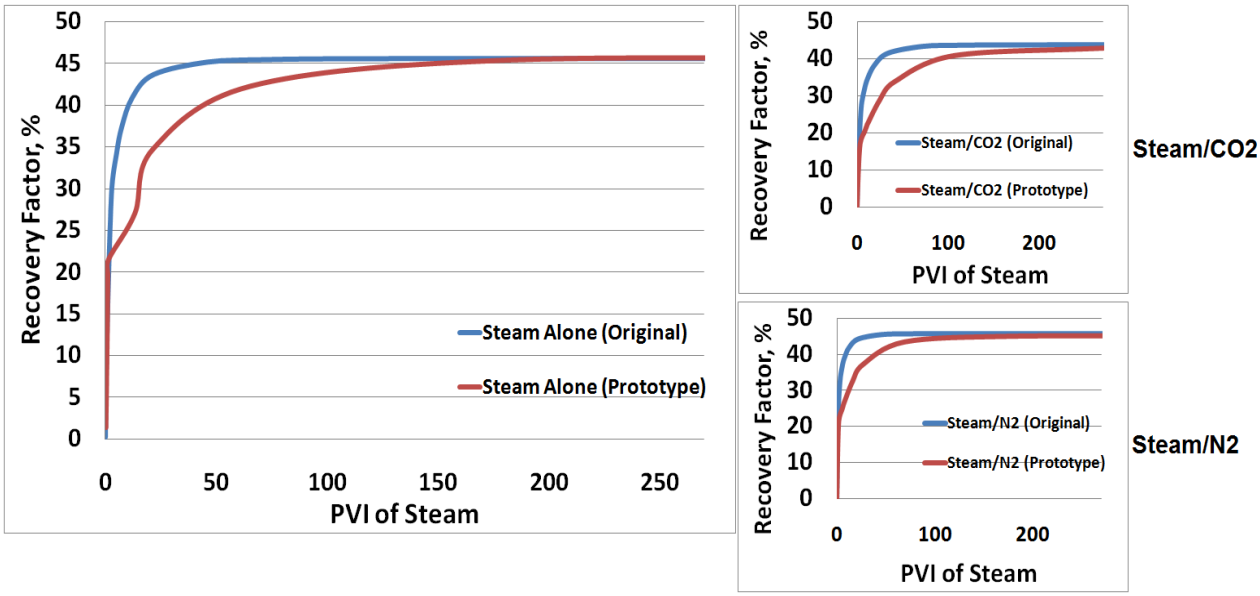

Figure 4-10: Recovery factor curves for prototype and original experiments.

Chapter 5

5. Experimental Modeling

This chapter presents the preparations made on prototype experiment including the experimental procedures and measurements. It also includes one plain steamflooding process experiment for the prototype experiment on heavy-oil. In addition, it discusses the preparations made for the long core, original experiment. The discussion, in this part, includes the basic core's petro-physical property measurements and introduces the CT scanning method of calculating the core's porosity. It also explains the saturation processes of brine and oil before the steamflooding process.

5.1. Short Core Experiment (Prototype)

5.1.1. CT Scanning System

The CT scanner, x-ray computed tomography, uses x-ray to capture multiphase fluid flow in porous media. It pictures the interior pores network and allows studying the fluids displacement pattern. CT scanner provides information of porosity, permeability and fluid phases distributions and hence very useful to implement in this study (Akin and Kovscek, 2003). Table 5-1-1 indicates the parameters used in the CT scan test.

Table 5-1-1: CT scan parameters.

Tube Current, mA	Energy Level, KeV	Exposure Time, sec/slice	Tickness, mm	Interval, mm
200	140	1	3	3

When an object is placed inside the CT scanner, the system obtains a complete set of data using an internal detector and converts them into images, in a process known as image reconstruction. Each produced pixel has a value of linear attenuation coefficient. The equipment converts all the coefficients into values known as CT number. Each material has its particular CT number. The CT numbers of air and Maloob oil are -1000 and 40.5 respectively. The CT number depends proportionally on the mass density. More details about the CT scanning system are found in (Akin and Kovscek, 2003). The images are processed using Tecplot 2009 RS software and reconstructed into 2-D and 3-D images.

As mentioned previously, the CT scanner allows the calculation of porosity and fluids saturations. The porosity is calculated as:

$$\phi = \frac{CT_{wr} - CT_{ar}}{CT_w - CT_a} \qquad \text{(Akin and Kovscek, 2003)} \quad (5\text{-}1)$$

where CT_{wr} is the CT number of water-saturated rock, CT_{ar} is the CT number of air-saturated rock, CT_w is the CT number of water and CT_a is the CT number of air.

When the core is originally saturated with water, the saturation profile is found as:

$$S_w = \frac{CT_{owr} - CT_{or}}{\phi(CT_w - CT_o)} \quad \text{(Akin and Kovscek, 2003)} \quad (5\text{-}2)$$

where S_w is the water saturation, ϕ is the rock porosity, CT_{owr} is the CT number of oil-water rock, CT_{or} is the CT number of oil-saturated rock and CT_o is the CT number of oil.

In addition, oil saturation profile is:

$$S_o = \frac{(CT_{owr} - CT_{wr})(1 - S_{wc})}{(CT_{swcr} - CT_{wr})} \quad \text{(Akin and Kovscek, 2003)} \quad (5\text{-}3)$$

where S_{wc} is the connate water saturation and CT_{swcr} is the CT number of connated water rock.

5.1.2. Cores Properties

The cores used in the analysis are taken from a heavy-oil field. The cores are carbonate type with vuggs and natural fractures with relatively low permeability and porosity values for the matrix. The cores are taken from a depth of 3128-3132ft. They are drilled in laboratory plugs using a drilling machine with 1.5 inches drilling bit for different lengths that sum up to 1 meter long cores. It is important to mention that the core selection process was based on availability and so there is a difference in quality of rocks used in the study. Quality refers to the petro-physical properties of the rocks. The study examines two experiments based on different core lengths; prototype and original experiments.

The cores used in prototype experiment are two cores with lengths of 1.9 inches and 1.6 inches, total of 3.5 inches. The measured permeability during the experiment is 0.514 mD. The average porosity of the cores is found using CT scanner and confirmed by volumetric calculations to be about 9.4%. For both cores, the CT scan analysis was helped by Elliot Kim. The images shown in Figure 5-1 indicate porosity values for different two-dimensional horizontal slices for both cores. Zones of high and low porosities are recognized by the color bar in the figure with dark blue indicating lowest porosity to red indicating the highest value. The slices show the core's pores network and hence rock morphology. Table 5-1-2 shows the core petro-physical properties.

Table 5-1-2: Core petro-physical properties.

Experiment	Length, inches	Test	Permeability, mD	Porosity, %	Temperautre, ^{o}F	Pressure Drop, psi
Prototype	3.5	100% synthetic brine with 3.1 wt% NaBr	0.516	9.4	131	70

In addition, initial water saturation and oil residual saturation were calculated using Equations 5-4 and 5-5.

$$S_{wi} = \frac{Water\ Volume\ In\ The\ Core}{Pore\ Volume} \quad (5\text{-}4)$$

$$S_{or} = (1\text{-}S_{wi}) \text{ x } (1\text{-Recovery Factor}) \quad (5\text{-}5)$$

The permeability is found using Darcy law,

$$K = \frac{q \cdot \mu \cdot L}{A \cdot \Delta P} \quad (5\text{-}6)$$

Table 5-1-3 lists the calculated parameters along with the brine and oil relative permeabilities at 150 F. The measured initial water and irreducible oil saturations, Sw_i and S_{ro}, are 0.283 and 0.423 respectively. The relative permeability values of oil and brine, k_{ro} and k_{rw}, are observed to be 0.87 and 0.0154 respectively.

Table 5-1-3: Fluids saturations and relative permeabilities.

Temp (^{o}C)	S_{wi}	S_{ro}	Permeability (mD)			K_{ro}	K_{rw}
			K	Ko_{eff}	Kw_{eff}		
70 (158^{o}F)	0.283	0.342	0.516	0.449	0.0079	0.87	0.0154

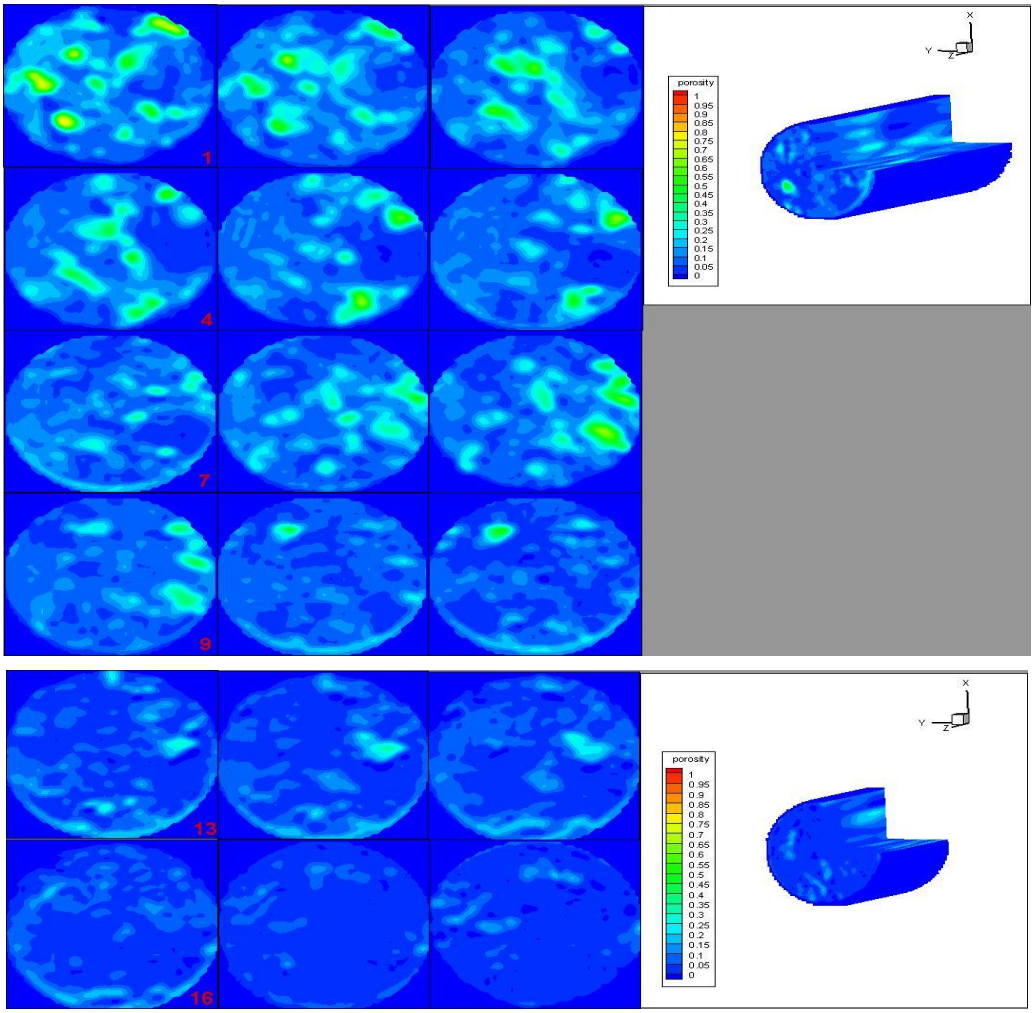

Figure 5-1: 2-D and 3-D images for porosity of the used sample.

5.1.3. Coreflood Preparation

Cores were drilled using a drilling machine with 1.5 inch diameter drill bit for different lengths that sum up to 1 meter long cores. Leaching process, then, took place to empty the cores from oil in which the cores are soaked in toluene for two days. The cores then are heated for one day until dryness using an oven with a temperature of 65.5^{o}C. The cores, then, are taped and stored in a closed area in the lab until experiment time.

When preparing the core-holder apparatus, the cores are placed on top of the metal bottom cap and are taped to hold the core along with the bottom cap, only the edge of the bottom core is tapped. The same occurs with the top cap and the cores edge. After that, heat sensitive polymeric tubes with 1:1.6 shrinking factor are used to cover the cores. The first layer of the shrinkable tubes is painted with silicone gel on the sides only and leaving the vuggs untouched. The tube, then, is placed around the cores where they shrink and confine the cores as hot air from the air blower is used to heat up the apparatus. After that, sufficient time, about two days, is given for the layer to dry. Figure

5-2 illustrates this stage. The second layer is fully painted from inside with silicone gel and placed around the first layer. A hot-air gun is used again to expose heat to the system and well attach the second layer. Again, the layer is left for two days to dry. A third, and final, layer is placed, heated and left to dry for two days.

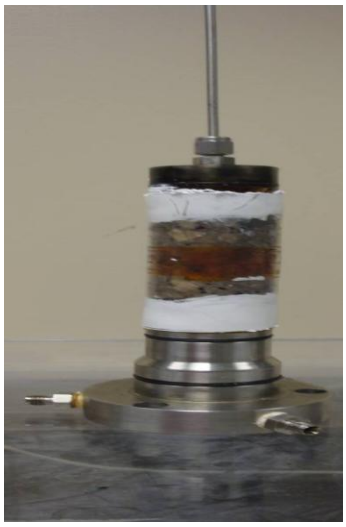

Figure 5-2: Cores preparation.

After that the apparatus is partially assembled and a check for any possible leak in the inside core system is run. The confining pressure is exerted using nitrogen and was increased to about 500 psi while a pressure gauge is placed on the entry point to detect any pressure leaking into the main stream. After that, the apparatus is left for about 6 hours and injection pressure is checked. If there is a leak into the system, the core holder must be dismantled and remade again. Else, the process of cleaning takes place ahead.

5.1.4. Cleaning Process

Before saturating the core with brine, it is necessary to clean the cores from any residual oil. The process relies on injecting three different solvents, one at a time, decane, isopropanol and toluene respectively. The solvent is injected into the system by a water pump. The water displaces the solvent from bottom as it has lighter density than water. Oil gets displaced and produced at the outlet. Every time a chemical is injected, oil production gets lesser until no sign of oil production is observed.

5.1.5. Brine Injection

The cores, after the cleaning process, were saturated with 100% synthetic brine. The injection pressure was about 70 psi and the temperature at 65.5^{o}C. The measured permeability, at this stage, is 0.5 mD and the porosity is 9.4%.

5.1.6. Oil Injection

Brine injection was followed by oil injection in which crude oil was injected into the core to saturate the pores at a low flowrate of 0.3ml/hr and a temperature of 65.5^0C. Due to the high viscosity nature of the oil, the injection process took about five days for the oil to be produced. The cores, then, were aged for several days. The calculated initial water saturation is 28% and the oil saturation is 72%.

5.1.7. Steam Injection

Prior to steam injection, the core holder was placed vertically in an oven to allow gravity effect on produced oil. The temperature of the oven is set to 150^0F, 65.5^oC. The steam is generated using a heating tape tightened around 1/8" line. It is difficult to control the steam quality using heating tapes and so steam temperature is raised to 400^0F at a pressure of 131psi increasing the visual certainty of a quality greater than 90%. The length of the extended steam line into the core is about 4 inches that has insignificant effect on steam quality reduction. The steam generator is shown in Figure 5-4. The steam temperature and pressure are monitored and controlled using proper temperature and pressure controllers. Water is used to confine the cores and the overburden pressure is 500 psi. Only the steam generator and the upstream back pressure regulator are outside the oven. The core holder and the downstream back pressure regulator are inside the oven as Figure 5-3 shows. Steam is injected at about 131psi into the core and produced at 15psi. Steam injection experiment lasted for approximately 100 hours in which no more oil was produced and water instead dropped out. Figure 5-5 shows the oven from inside with the coreflood equipment. Further details about the results are discussed in the next section.

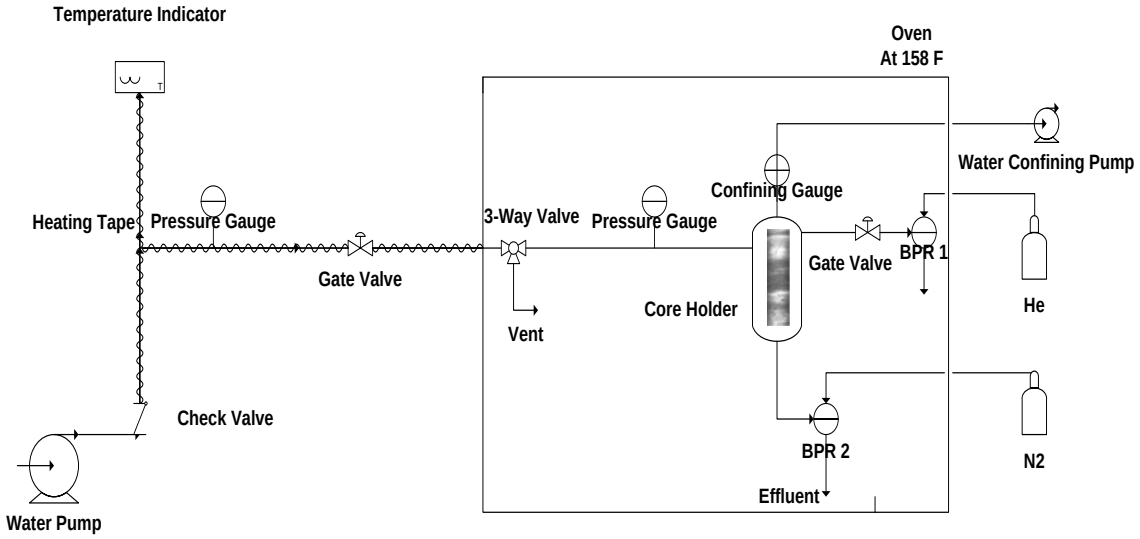

Figure 5-3: Coreflood experiment map.

Figure 5-4: Steam generator.

Figure 5-5: Inside the oven.

5.1.8. Steam Alone Injection Results

The experimental result presented in this section is steamflood process without non-condensable gas addition to the prototype core plugs with length of 3.5 inches and diameter of 1.5 inches. The injection process is non-isothermal. The experiment lasted for four days. The cumulative oil recovered at the end of the experiment has been plotted against time. Figure 5-6 shows how much oil was recovered from the oil originally in place during four days of steam injection.

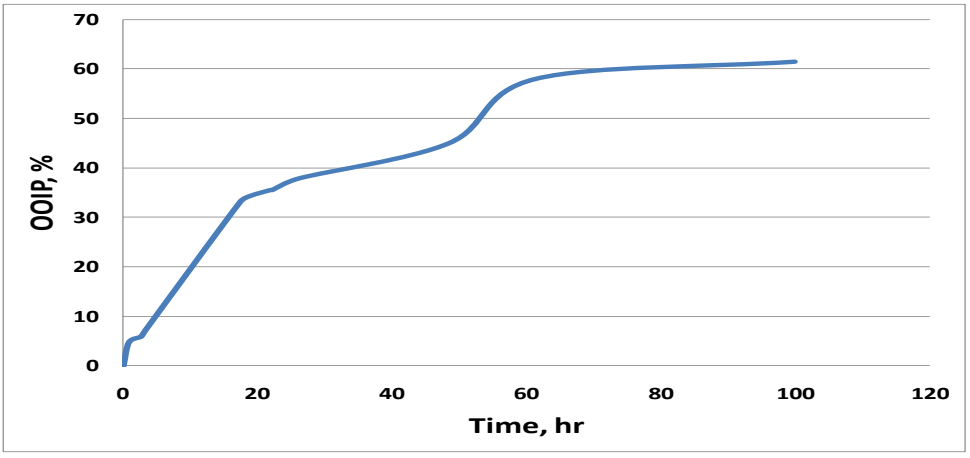

Figure 5-6: Oil recovery by experiment at 65.5°C.

As the graph indicates, the cumulative oil recovered is about 61.4% of oil originally in place. It can be seen from the graph different increasing humps. This may be attributed to two factors. First, the condensation rate of steam, i.e. the oil production occurred in three steps, one by steam, second by hot water from steam condensation and third by steam after hot water vaporized. Such a phenomenon is expected to yield a difference in the recovery trend because of the difference in the displacement patterns between hot water and steam when contacting the oil. The steam quality control was difficult during the experiment because of the humble setup used to generate steam that is discussed in the experimental section. This led steam quality at 348^{o}F at some point to drop after penetrating the cores at 150^{o}F that is, in fact, is expected. The second factor is the effect of forces controlling the production. The length of the cores is short, about 3.5 inches, and the permeability values are so small. These encourage the flow to be governed by capillarity. The injection pressure, however, is very large compared with the size of the cores. This will instigate the domination of the viscous force. Drawing a conclusion from a single experiment is difficult especially when no data about the exerted forces are yet available in hand. What exactly is the injection profile and how heat is distributed in the cores are yet to be answered.

5.2. Long Core Experiment (Original)

The design of the steam flood process is crucial for the given tight cores from Maloob field. The low petro-physical properties and the unconsolidated state of the rocks make the designing process unintuitive. This part explains the procedures of designing the steamflood process for the long core that consists of stacks of carbonate plugs with different lengths that sum up to 71cm.

The steam flood design process starts with the choice of proper core plugs that contain clear fractures and vuggs. Then, the cores are soaked in toluene for few days before soaking them in brine for similar period. The cores, after that, are aligned vertically very carefully. To ensure capillarity continuity, the plugs were separated by thin layers of smashed cores from the same field. This is shown in Figure 5-7. On the same way, the cores were aligned and taped with high temperature tape as shown in Figure 5-8. The cores were aligned, after that, using a heat shrinkable tube with silicone gel coated at the edges, Figure 5-9.

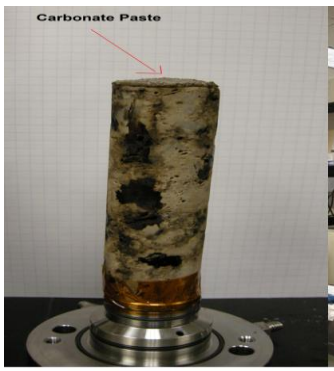


Figure 5-7: Carbonate paste. Figure 5-8: Aligned cores. Figure 5-9: Coated cores.

Then, another layer of the shrinkable tubes was entirely coated with the gel from inside and wrapped with foil to prevent gas escape. This is shown in Figure 5-10. The foil is then coated with the silicone gel and a third layer of the shrinkable tube is installed. This is shown in Figure 5-11. The final core holder apparatus is shown in Figure 5-12.

Figure 5-10: Wrapped core.

Figure 5-11: Fully coated core.

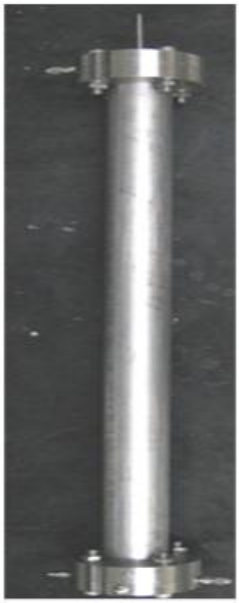

Figure 5-12: Core holder apparatus.

After setting up the core holder, a confining pressure test using nitrogen gas is necessary to trace possible leaks in the system. When leak is detected in the system, it is usually due to poor layering of the shrinkable tubes or damages on the o-rings of the metal caps. The regular procedure when leak is detected suggests the removal of the entire layers and the re-installment of the layers again. The system when tested showed a clear leak from the first run. This is always expected but even more for this particular design since this is the first time to implement it in the group. Therefore, a new modification had to be made on the metal cap in order to support the long core and prevent any possible shaking that tends to let the gas leak through. Figure 5-13 shows the modified piece. The metal cab was extended about 5.6cm to support the confining of the core.

Figure 5-13: Modified bottom cap.

5.2.1. Air Permeability Calculations

The core was vacuumed initially for about five days to insure complete dryness. Then air was injected at 100psi pressure drop. It took about 45 mins for the air to exit from the producer side. This gives a quick hint of how small is the total average permeability of the rock used. The air flowrate was calculated using bubble flow meter 2.3 cc/min. Using Darcy law for gases, the average permeability of air was found to be 0.176 mD.

5.2.2. Core Porosity Calculations

After calculating the air permeability of the long core, the core was saturated with air at 100psi and CT scan images were taken, a picture of every 1 cm. Then, CO_2 gas was injected and air was displaced at room temperature. The core was again saturated but this time with CO_2 at 100psi. CT scan images were taken for the same number of slices. The saturation of gases took place while the core was confined with water at 400 psi. After getting the images of the core for the two gases, the average CT numbers were calculated for every slice. Then, with the knowledge of the CT number of pure air and CO2 at room temperature and 100psi, the porosity values for every slice were calculated using Equation 5-7.

$$\phi = \frac{CT_{CO2,rock} - CT_{air,rock}}{CT_{CO2,pure} - CT_{air,pure}} \tag{5-7}$$

The values, then, were averaged to correspond to the total average porosity of the long core that is about 9.96%.

This is the point where the experimental work stopped. The experiment is expected to continue even after this documentation to study the effect of steam/N_2 on oil recovery by gravity drainage and compare the results with another run of steam alone injection.

Chapter 6

6. Conclusion and Future Work

This work reached several conclusions about the effectiveness of adding condensable gas, CO_2, and non-condensable gas, N_2, during steamflood process on heavy-oil recovery. It was found in all numerical experiments that the addition of nitrogen gas improved slightly the oil recovery over steam alone injection. The improvement is attributed to the early channeling of the gas in the formation before steam front becomes stable that improved the sweep of the reservoir. It is the early gas penetration that made the improvement. Carbon dioxide when added as a condensable gas to steamflood increased the recovery at early time over steam injection. The production, however, decreased slightly afterwards and the ultimate oil recovered was less when compared to steam and steam/N_2 floods. This is attributed to the heating profile at early times where CO_2 enters the formation earlier than steam forcing a drive on the oil but as the concentration of the gas increases the recovery starts to decrease. This is due to the decrease in steam volume as the gas concentration increases. In the steam/N_2 case, the heat provided to the formation is the highest compared to steam and steam/CO_2. This is because the concentration of the N_2 increased to about 100% in the first day leaving very minimal concentration of steam in the formation. As time passes, the steam concentration starts to increase gradually while the nitrogen concentration decreases to reach almost 0. Then, the steam/N_2 injection temperature exceeds the steam saturation temperature and the pressure starts to decrease indicating the increase in steam volume in the formation. The difference between the roles of CO_2 and N_2 may be attributed to the fact that CO_2 is soluble in oil and water while N_2 is not. If CO_2 co-injection is treated as non-condensable gas, it would act similar to N_2 when co-injected with steam. It is recommended, therefore, to inject non-condensable gas with steam over condensable gas injection.

The early breakthrough is a property of the added gas whether it was condensable or non-condensable gas. The breakthrough of the non-condensable gas is earlier than the breakthrough of the condensable gas.

The production increases as the oil gravity increases due to gravity drainage effect at lower oil viscosities. At lower oil viscosities, the steam and the gas penetrate the formation faster than at greater oil viscosities leading to earlier heating and pushing drive to the oil as well as breakthrough. The injection profile becomes more stable for greater gravities. This includes steam alone, steam/CO_2 and steam/N_2 injections

The recovery is relatively less improved by the addition of condensable CO_2 for oil with greater gravities due to the decrease in the gas solubility in oil as the temperature increases. The effect of adding N_2 on lighter oil gravities is represented in supporting the driving pressure and providing the extra heating brought by the increase in steam volume resulted from steam partial pressure reduction.

It was also found that the greater the CO_2 concentration, the less the recovery becomes. The recovery, however, when injecting N_2 is almost the same for different concentrations.

In addition, when injecting the steam/gas at temperature greater than steam saturated temperature, no additional improvements on recovery is observed. This is because the heat that contributes toward heating the reservoir is the steam latent heat of vaporization and not the sensible heat. Therefore, superheating steam may have very minimal effect on recovery. Steam temperature variations have larger effect on CO_2 than N_2 due to the solubility difference between the gases.

In the future, the experimental work will continue in order to match the results with the simulation results. The prototype experiments will include steam, steam/CO_2 and steam/N_2 injections. The original experiments will include steam and steam/N_2 injections.

Nomenclature

A: Cross-sectional Area
CT_{wr}: The CT number of water-saturated rock
CT_{ar}: The CT number of air-saturated rock
CT_{w}: The CT number of water
CT_{a}: The CT number of air.
CT_{owr}: The CT number of oil-water rock
CT_{or}: The CT number of oil-saturated rock
CT_{o}: The CT number of oil
CT_{swcr}: The CT number of connated water rock
g: Gravity acceleration
H: Height of the top of the 100% saturated region after reaching equilibrium
h: Height of the top of the 100% saturated region before reaching equilibrium
k: Permeability of the medium to the fluid
$\vec{\vec{k}}$ is the permeability tensor
L: Core Length
μ: Fluid viscosity
ρ: Fluid density
p: Fluid pressure
P_k: Pressure of phase k
ΔP: Pressure Drop
ρ_k: Density of phase k
$\frac{\partial p}{\partial z}$: Pressure gradient
q: Fluid flow rate
S_{or}: Average residual oil saturation after time t
S_w: Water saturation
S_{wi}: Initial Water Saturation
S_{wc}: The connated water saturation
$\vec{u}_k$: Darcy velocity in k direction
v: Macroscopic fluid velocity downward
v_u: Velocity in the partially saturated region
v_s: Velocity in the fully saturated region
ν_s: Kinematic viscosity of the oil at steam temperature
ξ: Fractional saturation, the variable upon which the pressure, p, depends
φ: Rock Porosity
$\vec{\nabla}$: Divergence operator
λ_{rk}: Mobility ratio of k phase

References

Aherne, A. L., Birrell, G. E., 2002. "Observations Relating to Non-Condensable Gasses in a Vapour Chamber: Phase B of the Dover Project", paper SPE 79023 prepared for presentation at the 2002 SPE International Thermal Operations and Heavy Oil Symposium and International Horizontal Well Technology Conference, Calgary, Canada, November 4-7.

Akin, S., Kovscek, A., "Computed Tomography in Petroleum Engineering Research" Geological Society, London, Special Publications 2003; v. 215; p. 23-38.

Bader, B. E., Fox, R. L., and Stosur, J. J. , 1979. "The Potential of Downhole Steam Generation to the Recovery of Heavy Oils" presented at UNITAR First International Conference on the Future of Heavy Crude and Tar Sand, Edmonton.

Bagci, A. S., Gumrah, F., 2004. "Effects of CO_2 and CH_4 Addition to Steam on Recovery of West Kozluca Heavy Oil", paper SPE 86953 prepared for presentation at the 2004 SPE International Thermal Operations and Heavy Oil Symposium and Western Regional Meeting, Bakersfield, CA., March 16-18.

Butler, R.M., 1991. Thermal Recovery of Oil and Bitumen, Prentice Hall, Englewood Cliffs, New Jersey. (p 122-123)

Butler, R., Jiang, Q., Yee, C., 1999. "Steam and Gas Push (SAGP) Recent Theoretical Developments and Laboratory Results" paper presented at the CSPG and Petroleum Society Joint Convention, Digging Deeper, Finding a Better Bottom Line, Calgary, Alberta, Canada, June 14-18, 1999.

Canbolat S. , Akin S. , Kovscek A. R, "Noncondensable Gas Steam-Assisted Gravity Drainage" Journal of Petroleum Science and Engineering, 45, (2004), p.83-96

Cardwell, Jr., W., Parsons, R., "Gravity Drainage Theory", AIME paper presented in Dallas and Los Angeles Meetings, October 1948

Clampitt, R. L., Eson, R. L., Cooke, R. W., 1991. "Applying a Novel Steam-CO_2 Combination Process in Heavy Oil and Tar Sands", paper SPE 21547 prepared for presentation at the International Thermal Operations Symposium, Bakersfield, CA., February 7-8.

Garattoni, C., Jing, X., Dawe, R., "Dimensionless Groups For Three-Phase Gravity Drainage Flow In Porous Media" Journal of Petroleum Science and Engineering 29 (2001) 53-65.

Hong, K.C., Ault, J. W., 1984. "Effects of Noncondensable Gas Injection on Oil Recovery by Steamflooding", paper SPE 11702 presented at the 1983 SPE California Regional Meeting, Ventura, CA., March 23-25.

Hutchinson, H. L., Lp, D. T., Shirazi, M., 1983. "Experimental Study of Coinjection of Steam With Air or Other Coinjections Into Asphalt Ridge Tar Sands", paper SPE 11850 presented at the Rocky Mountain Regional Meeting, Salt Lake City, UT., May 23-25.

Hornbrook M. W., Kaveh Dehghanl, Suhail Qadeer, R.D. Ostermann, 1989. "Effects of CO_2 Addition to Steam on Recovery of West Sak Crude Oil" paper SPE 18753 presented at the 1989 SPE California Regional Meeting held in Bakersfield, April 5-7

Harding T. G. ,Farouq Ali S.M. ,Flock D.L , 1983. "Steamflood Performance in The Presence of Carbon Dioxide and Nitrogen" Journal of Canadian Petroleum Technology, (Sept.-Oct. 1983), pp. 30-37

Jacobs, F. A., Donnelly, J. K., Stanislav, J.S., and Svrcek, W. Y., 1980. "Viscosity of Gas-Saturated Bitumen" Journal of Canadian Petroleum Technology, (Oct.-Dec. 1980), Vol. 19, No 4, pp.46-50

Lake, L. W., 1989. Enhanced Oil Recovery, Prentice Hall, Englewood Cliffs, New Jersey. (p 461-463)

Louis C. Leung, 1983. "Numerical Evaluation of the Effect of Simultaneous Steam and Carbon Dioxide Injection on the Recovery of Heavy Oil" paper SPE 10776 presented at the 1982 SPE California Regional Meeting held in San Francisco, March 4-26

Moussine, K., Ibragimov, N., Khisamov, R., 2007. "The Optimization of Gas/Steam Injection Using Numerical Simulation" paper SPE 105199 prepared for presentation at the 15th SPE Middle East Oil & Gas Show and Conference, Bahrain International Exhibition Centre, Kingdom of Bahrain, March 11-14.

Pursley, S. A., 1975. "Experimental Studies of Thermal Recovery Processes" paper presented at the Maracaibo Heavy Oil Symposium, Maracaibo, Venezuela, June 4.

Redford, D. A., 1982. "The Use of Solvents and Gases with Steam in The Recovery of Bitumen from Oil Sands" JCPT, (January-February), 45-53.

Appendix A

A. Reservoir Simulation Model Codes

A.1. Steam Alone Base Case Model

```
**----------------------INPUT-OUTPUT CONTROL----------------------------------------
*INUNIT *field
*OUTUNIT *field
**-------------------------RESERVOIR DESCRIPTION-----------------------------------
*GRID *CART 11 1 50
*di *ivar 0.5 0.033 3*0.5 0.033 3*0.5 0.033 0.5
*dj *con 0.5
*dk *con  0.2
*KDIR *DOWN
*POR *con 0.25
*PERMI *con 50
*PERMJ *con 50
*PERMK *IJK 1:11 1 1:50 20
*IJK 2 1 1:50 8000
*IJK 6 1 1:50 8000
*IJK 10 1 1:50 8000
*end-grid
*CPOR 5e-4
*CTPOR 0
*rockcp 35.02
*thconr 106
*thconw 0.36
*thcono 0.077
*thcong 0.0833
**--------------------------COMPONENT PROPERTIES-------------------------------------
*MODEL 4 4 4
*COMPNAME       'WATER'    'HEVY OIL' 'LITE OIL' 'MEDM OIL'
**                          -----          -------         --------        --------
   *CMM        18.02      600 250       450
   *PCRIT      3206.2      0  225       140
   *TCRIT      705.4       0         800        950
   *AVG        1.13e-5     0         5.e-5      1.e-4
   *BVG        1.075       0         0.9        0.9
   *MOLDEN     0        0.10113      0.2092      0.1281
   *CP         0        0.000005     0.000015            0
   *CT1        0        0.00038      0.00114                      0
   *CPL1       0        300          132.5      247.5
   ** Two volatile oils and one dead oil
   *kv1        0           0        8.334e8    1.554e5
   *kv3        0           0        1.23e6       212
   *kv4        0           0        -16000     -4000
   *kv5        0           0        -460         20
*VISCTABLE
**      Temp
        75     0       40828.8     2.328      10.583
       100     0       13489.8     1.9935      9.061
       150     0       1092.4      1.4905      6.775
       200     0       130.3       1.1403      5.183
       250     0       60.6        0.8896      4.0434
       300     0       31          0.7058      3.2082
       350     0       17.9        0.5683      2.5833
       400     0        10         0.4754      2.0383
               450     0      6                 0.4053   1.5765
**-----------------------------------ROCK~FLUID DATA----------------------------------
```

```
*rockfluid
RPT 1
*swt   **  Water-oil relative permeabilities
** Sw                    krw                 kro                 Pcow
0                       0           0.87                24
0.027777778             5.95E-07            0.821703443         16
0.097222222             8.93E-05            0.702354595         5.8
0.166666667             0.000771605         0.587384259         4.8
0.236111111             0.00310789          0.479366126         3.2
0.305555556             0.008716873         0.380388285         2.7
0.375                   0.019775391         0.292053223         2.3
0.444444444             0.039018442         0.215477824         2.1
0.513888889             0.069739192         0.15129337          1.9
0.583333333             0.115788966         0.099645544         1.8
0.652777778             0.181577255         0.060194423         1.5
0.722222222             0.272071712         0.032114483         1
0.791666667             0.392798153         0.0140946           0
0.861111111             0.549840559         0.004338045         0
0.930555556             0.749841072         0.000562489         0
1                       1                   0                   0
*slt    **  Oil-gas relative permeabilities
**   Sl                 Krg                 Krog                Pcog
**  ----                -------     -------     -----
0.34                    1                   0                   0
0.4                     0.826               0.008               0
0.45                    0.694               0.028               0
0.5                     0.574               0.059               0
0.55                    0.465               0.101               0
0.6                     0.367               0.155               0
0.65                    0.281               0.221               0
0.7                     0.207               0.298               0
0.75                    0.143               0.386               0
0.8                     0.092               0.486               0
0.85                    0.052               0.597               0
0.9                     0.023               0.72                0
0.95                    0.006               0.79                0
1                       0                   0.87                0
**----------------------------------INITIAL CONDIRION---------------------------------------
*initial
VERTICAL DEPTH_AVE
INITREGION 1
REFPRES 132
REFBLOCK 1 1 50
*sw *con 0.28
*so *con 0.72
*temp *con 150.
*mfrac_oil 'LITE OIL' *con  0.01
*mfrac_oil 'MEDM OIL' *con  0.02
*mfrac_oil 'HEVY OIL' *con  0.97
**----------------------------------NUMERICAL CONTROL---------------------------------------
*NUMERICAL
*RUN
**----------------------------------RECURRENT DATA-------------------------------------------
time 0
DTWELL 0.05
**
**
**
**    well 1 'INJECTOR'
**$
WELL 1  'INJECTOR 1'
                    ** mole fraction of water (steam) injected
INJECTOR MOBWEIGHT 'INJECTOR 1'
INCOMP  WATER  1  0.0 0.0 0.0
TINJW 360
QUAL  0.9
OPERATE  MAX  BHP  150.  CONT
**$         rad  geofac  wfrac  skin
GEOMETRY  K  0.5  1.  1.  0.
PERF  TUBE-END  'INJECTOR 1'
```

```
**$ UBA    ff  Status  Connection
   1 1 1  1.  OPEN    FLOW-FROM  'SURFACE'
** **
** **
** WELL 2  'INJECTOR 2'
**$
WELL  'INJECTOR 2'
                ** mole fraction of water (steam) injected
INJECTOR MOBWEIGHT 'INJECTOR 2'
INCOMP  WATER  1  0.0 0.0 0.0
TINJW 360
QUAL  0.9

OPERATE  MAX  BHP 150  CONT
*GEOMETRY *K 0.50 1 1 0
*PERF *TUBE-END 'INJECTOR 2'
    2 1 1 1.00
**
**
WELL 3  'INJECTOR 3'
                ** mole fraction of water (steam) injected
INJECTOR MOBWEIGHT 'INJECTOR 3'
INCOMP  WATER  1  0.0 0.0 0.0
TINJW 360
QUAL  0.9
OPERATE  MAX  BHP 150  CONT
*GEOMETRY *K 0.50 1 1 0
*PERF *TUBE-END 'INJECTOR 3'
    3 1 1 1.00
**
**
WELL 4  'INJECTOR 4'
                ** mole fraction of water (steam) injected
INJECTOR MOBWEIGHT 'INJECTOR 4'
INCOMP  WATER  1  0.0 0.0 0.0
TINJW 360
QUAL  0.9
OPERATE  MAX  BHP 150  CONT
*GEOMETRY *K 0.50 1 1 0
*PERF *TUBE-END 'INJECTOR 4'
    4 1 1 1.00
**
**
WELL 5  'INJECTOR 5'
                ** mole fraction of water (steam) injected
INJECTOR MOBWEIGHT 'INJECTOR 5'
INCOMP  WATER  1  0.0 0.0 0.0
TINJW 360
QUAL  0.9
OPERATE  MAX  BHP 150  CONT
*GEOMETRY *K 0.50 1 1 0
*PERF *TUBE-END 'INJECTOR 5'
    5 1 1 1.00
**
**
WELL 6  'INJECTOR 6'
                ** mole fraction of water (steam) injected
INJECTOR MOBWEIGHT 'INJECTOR 6'
INCOMP  WATER  1  0.0 0.0 0.0
TINJW 360
QUAL  0.9
OPERATE  MAX  BHP 150  CONT
*GEOMETRY *K 0.50 1 1 0
*PERF *TUBE-END 'INJECTOR 6'
    6 1 1 1.00
**
**
WELL 7  'INJECTOR 7'
                ** mole fraction of water (steam) injected
INJECTOR MOBWEIGHT 'INJECTOR 7'
```

```
INCOMP  WATER  1  0.0 0.0 0.0
TINJW 360
QUAL  0.9
OPERATE  MAX  BHP 150  CONT
*GEOMETRY *K 0.50 1 1 0
*PERF *TUBE-END 'INJECTOR 7'
     7 1 1 1.00
**
**
WELL 8  'INJECTOR 8'
                    ** mole fraction of water (steam) injected
INJECTOR MOBWEIGHT 'INJECTOR 8'
INCOMP  WATER  1  0.0 0.0 0.0
TINJW 360
QUAL  0.9
OPERATE  MAX  BHP 150  CONT
*GEOMETRY *K 0.50 1 1 0
*PERF *TUBE-END 'INJECTOR 8'
     8 1 1 1.00
**
**
WELL 9  'INJECTOR 9'
                    ** mole fraction of water (steam) injected
INJECTOR MOBWEIGHT 'INJECTOR 9'
INCOMP  WATER  1  0.0 0.0 0.0
TINJW 360
QUAL  0.9
OPERATE  MAX  BHP  150.  CONT
**$          rad  geofac  wfrac  skin
GEOMETRY  K  0.5  1.  1.  0.
PERF  TUBE-END  'INJECTOR 9'
**$ UBA     ff  Status  Connection
   9 1 1  1.  OPEN    FLOW-FROM  'SURFACE'
**
**
WELL 10  'INJECTOR 10'
                    ** mole fraction of water (steam) injected
INJECTOR MOBWEIGHT 'INJECTOR 10'
INCOMP  WATER  1  0.0 0.0 0.0
TINJW 360
QUAL  0.9
OPERATE  MAX  BHP 150  CONT
*GEOMETRY *K 0.50 1 1 0
*PERF *TUBE-END 'INJECTOR 10'
**$ UBA     ff  Status  Connection
   10 1 1  1.  OPEN    FLOW-FROM  'SURFACE'
**
**
WELL 11  'INJECTOR 11'
                    ** mole fraction of water (steam) injected
INJECTOR MOBWEIGHT 'INJECTOR 11'
INCOMP  WATER  1  0.0 0.0 0.0
TINJW 360
QUAL  0.9
OPERATE  MAX  BHP 150  CONT
*GEOMETRY *K 0.50 1 1 0
*PERF *TUBE-END 'INJECTOR 11'
     11 1 1 1.00
**
**
**    well 12 'PRODUCER 1'
**$
WELL 12 'PRODUCER 1'
PRODUCER 'PRODUCER 1'
OPERATE  MIN  BHP  132  CONT REPEAT
                      ** i  j  k
**$          rad  geofac  wfrac  skin
*GEOMETRY *K 0.50 1 1 0
PERF  TUBE-END  'PRODUCER 1'
**$ UBA     ff  Status  Connection
```

```
   1 1 50  1.  OPEN    FLOW-TO  'SURFACE'
**
**
**    well 13 'PRODUCER 2'
**$
WELL 13 'PRODUCER 2'
PRODUCER 'PRODUCER 2'
OPERATE  MIN  BHP  132  CONT REPEAT
                     ** i  j  k
**$         rad  geofac  wfrac  skin
*GEOMETRY *K 0.50 1 1 0
*PERF *TUBE-END 'PRODUCER 2'
    2 1 50 1.00
**
**
**    well 14 'PRODUCER 3'
**$
WELL 14 'PRODUCER 3'
PRODUCER 'PRODUCER 3'
OPERATE  MIN  BHP  132  CONT REPEAT
                     ** i  j  k
**$         rad  geofac  wfrac  skin
*GEOMETRY *K 0.50 1 1 0
*PERF *TUBE-END 'PRODUCER 3'
    3 1 50 1.00
**
**
**    well 15 'PRODUCER 4'
**$
WELL 15 'PRODUCER 4'
PRODUCER 'PRODUCER 4'
OPERATE  MIN  BHP  132  CONT REPEAT
                     ** i  j  k
**$         rad  geofac  wfrac  skin
*GEOMETRY *K 0.50 1 1 0
*PERF *TUBE-END 'PRODUCER 4'
    4 1 50 1.00
**
**
**    well 16 'PRODUCER 5'
**$
WELL 16 'PRODUCER 5'
PRODUCER 'PRODUCER 5'
OPERATE  MIN  BHP  132  CONT REPEAT
                     ** i  j  k
**$         rad  geofac  wfrac  skin
*GEOMETRY *K 0.50 1 1 0
*PERF *TUBE-END 'PRODUCER 5'
    5 1 50 1.00
**
**
**    well 17 'PRODUCER 6'
**$8
WELL 17 'PRODUCER 6'
PRODUCER 'PRODUCER 6'
OPERATE  MIN  BHP  132  CONT REPEAT
                     ** i  j  k
**$         rad  geofac  wfrac  skin
*GEOMETRY *K 0.50 1 1 0
*PERF *TUBE-END 'PRODUCER 6'
    6 1 50 1.00
**
**
**    well 18 'PRODUCER 7'
**$
WELL 18 'PRODUCER 7'
PRODUCER 'PRODUCER 7'
OPERATE  MIN  BHP  132  CONT REPEAT
                     ** i  j  k
**$         rad  geofac  wfrac  skin
```

```
*GEOMETRY *K 0.50 1 1 0
*PERF *TUBE-END 'PRODUCER 7'
    7 1 50 1.00
**
**
**    well 19 'PRODUCER 8'
**$
WELL 19 'PRODUCER 8'
PRODUCER 'PRODUCER 8'
OPERATE  MIN  BHP  132  CONT REPEAT
                     ** i  j  k
**$         rad  geofac  wfrac  skin
*GEOMETRY *K 0.50 1 1 0
*PERF *TUBE-END 'PRODUCER 8'
    8 1 50 1.00
**
**
**    well 20 'PRODUCER 9'
**$
WELL 20 'PRODUCER 9'
PRODUCER 'PRODUCER 9'
OPERATE  MIN  BHP  132  CONT REPEAT
                     ** i  j  k
**$         rad  geofac  wfrac  skin
*GEOMETRY *K 0.50 1 1 0
*PERF *TUBE-END 'PRODUCER 9'
    9 1 50 1.00
**
**
**    well 21 'PRODUCER 10'
**$
WELL 21 'PRODUCER 10'
PRODUCER 'PRODUCER 10'
OPERATE  MIN  BHP  132  CONT REPEAT
                     ** i  j  k
**$         rad  geofac  wfrac  skin
*GEOMETRY *K 0.50 1 1 0
*PERF *TUBE-END 'PRODUCER 10'
    10 1 50 1.00
**
**
**    well 22 'PRODUCER 11'
**$
WELL 22 'PRODUCER 11'
PRODUCER 'PRODUCER 11'
OPERATE  MIN  BHP  132  CONT REPEAT
                     ** i  j  k
**$         rad  geofac  wfrac  skin
GEOMETRY  K  0.5  1.  1.  0.
PERF  TUBE-END  'PRODUCER 11'
**$ UBA      ff  Status  Connection
   11 1 50  1.  OPEN    FLOW-TO  'SURFACE'
**
*TIME 1
*TIME 2
*TIME 3
*TIME 4
*TIME 5
*TIME 6
*TIME 7
*TIME 8
*TIME 9
*TIME 10
*TIME 11
*TIME 12
*TIME 13
*TIME 14
*TIME 15
*TIME 16
*TIME 17
```

```
*TIME 18
*TIME 19
*TIME 20
*TIME 21
*TIME 22
*TIME 23
*TIME 24
*TIME 25
*TIME 26
*TIME 27
*TIME 28
*TIME 29
*TIME 30
*TIME 40
*TIME 50
*TIME 60
*TIME 70
*TIME 150
*TIME 300
*STOP
```

A.2. Steam/N_2 Base Case Model

```
**----------------------INPUT-OUTPUT CONTROL----------------------------------------
*INUNIT *field
*OUTUNIT *field
**------------------------RESERVOIR DESCRIPTION-----------------------------------
*GRID *CART 11 1 50
*di *ivar 0.5 0.033 3*0.5 0.033 3*0.5 0.033 0.5
*dj *con 0.5
*dk *con  0.2
*KDIR *DOWN
*POR *con 0.25
*PERMI *con 50
*PERMJ *con 50
*PERMK *IJK 1:11 1 1:50 20
*IJK 2 1 1:50 8000
*IJK 6 1 1:50 8000
*IJK 10 1 1:50 8000
*end-grid
*CPOR 5e-4
*CTPOR 0
*rockcp 35.02
*thconr 106
*thconw 0.36
*thcono 0.077
*thcong 0.0833
**--------------------------COMPONENT PROPERTIES-----------------------------------
*MODEL 5 5 4
*COMPNAME      'WATER'    'HEVY OIL'   'LITE OIL' 'MEDM OIL'     'N2'
**             -----     -------              --------  --------         ------
   *CMM       18.02     600          250       450               28
   *PCRIT     3206.2    0        225       140       492.4
   *TCRIT     705.4     0        800       950          -147
   *AVG       1.13e-5   0        5.e-5     1.e-4                0.042
   *BVG       1.075     0        0.9       0.9          0
   *MOLDEN    0       0.10113     0.2092     0.1281
```

```
   *CP       0      0.000005    0.000015          0
   *CT1      0      0.00038     0.00114       0
   *CPL1     0      300         132.5     247.5     0
   ** Two volatile oils and one dead oil
   *kv1      0        0       8.334e8   1.554e5
   *kv3      0        0       1.23e6      212
   *kv4      0        0       -16000      -4000
   *kv5      0        0       -460        20
*VISCTABLE
**      Temp
        75.0    0.0     40828.8       2.328     10.583
        100.0   0.0     13489.8       1.9935    9.061
        150.0   0.0     1092.4        1.4905    6.775
        200.0   0.0     130.3         1.1403    5.183
        250.0   0.0     60.6          0.8896    4.0434
        300.0   0.0     31.0          0.7058    3.2082
        350.0   0.0     17.9          0.5683    2.5833
        400.0   0.0     10.0          0.4754    2.0383
              450     0         6           0.4053    1.5765
**----------------------------------ROCK~FLUID DATA----------------------------------------
*rockfluid
RPT 1
*swt   **  Water-oil relative permeabilities
** Sw                  krw                 kro             Pcow
0                               0           0.87                24
0.027777778                     5.95E-07            0.821703443                     16
0.097222222                     8.93E-05            0.702354595                     5.8
0.166666667                     0.000771605                 0.587384259                     4.8
0.236111111                     0.00310789                  0.479366126                     3.2
0.305555556                     0.008716873                 0.380388285                     2.7
0.375                           0.019775391                 0.292053223                     2.3
0.444444444                     0.039018442                 0.215477824                     2.1
0.513888889                     0.069739192                 0.15129337                      1.9
0.583333333                     0.115788966                 0.099645544                     1.8
0.652777778                     0.181577255                 0.060194423                     1.5
0.722222222                     0.272071712                 0.032114483                     1
0.791666667                     0.392798153                 0.0140946                   0
0.861111111                     0.549840559                 0.004338045                     0
0.930555556                     0.749841072                 0.000562489                     0
1                               1                           0                               0
*slt   **  Oil-gas relative permeabilities
**  Sl                  Krg                 Krog                Pcog
** ----                 -------     -------     -----
0.34                            1                   0               0
0.4                             0.826               0.008           0
0.45                            0.694               0.028           0
0.5                             0.574               0.059           0
0.55                            0.465               0.101           0
0.6                             0.367               0.155           0
0.65                            0.281               0.221           0
0.7                             0.207               0.298           0
0.75                            0.143               0.386           0
0.8                             0.092               0.486           0
0.85                            0.052               0.597           0
0.9                             0.023               0.72            0
0.95                            0.006               0.79            0
1                               0                   0.87            0
```

```
**----------------------------------INITIAL CONDIRION----------------------------------------
*initial
VERTICAL DEPTH_AVE
INITREGION 1
REFPRES 132
REFBLOCK 1 1 50
*sw *con 0.28
*so *con 0.72
*temp *con 150.
*mfrac_oil 'LITE OIL' *con  0.01
*mfrac_oil 'MEDM OIL' *con  0.02
*mfrac_oil 'HEVY OIL' *con  0.97
**----------------------------------NUMERICAL CONTROL----------------------------------------
*NUMERICAL
*RUN
**----------------------------------RECURRENT DATA-------------------------------------------
time 0
DTWELL 0.05
**
WELL 1  'INJECTOR 1'
                ** mole fraction of water (steam) injected
INJECTOR MOBWEIGHT 'INJECTOR 1'
INCOMP  WATER-GAS  0.75  0.  0.  0.  0.25
TINJW  337.
QUAL  0.9
OPERATE  MAX  BHP  150.  CONT
**$        rad  geofac  wfrac  skin
GEOMETRY  K  0.5  1.  1.  0.
PERF  TUBE-END  'INJECTOR 1'
**$ UBA    ff  Status  Connection
   1 1 1  1.  OPEN    FLOW-FROM  'SURFACE'
** **
** **
WELL  'INJECTOR 2'
                ** mole fraction of water (steam) injected
INJECTOR MOBWEIGHT EXPLICIT 'INJECTOR 2'
INCOMP  WATER-GAS  0.75  0.  0.  0.  0.25
TINJW  337.
QUAL  0.9
OPERATE  MAX  BHP  150.  CONT
**$        rad  geofac  wfrac  skin
GEOMETRY  K  0.5  1.  1.  0.
PERF  TUBE-END  'INJECTOR 2'
**$ UBA    ff  Status  Connection
   2 1 1  1.  OPEN    FLOW-FROM  'SURFACE'
**
** **
WELL  'INJECTOR 3'
                ** mole fraction of water (steam) injected
INJECTOR MOBWEIGHT EXPLICIT 'INJECTOR 3'
INCOMP  WATER-GAS  0.75  0.  0.  0.  0.25
TINJW  337.
QUAL  0.9
OPERATE  MAX  BHP  150.  CONT
**$        rad  geofac  wfrac  skin
GEOMETRY  K  0.5  1.  1.  0.
PERF  TUBE-END  'INJECTOR 3'
```

```
**$ UBA    ff  Status  Connection
   3 1 1  1.  OPEN    FLOW-FROM  'SURFACE'
** **
** **
WELL  'INJECTOR 4'
                  ** mole fraction of water (steam) injected
INJECTOR MOBWEIGHT EXPLICIT 'INJECTOR 4'
INCOMP  WATER-GAS  0.75  0.  0.  0.  0.25
TINJW  337.
QUAL  0.9
OPERATE  MAX  BHP  150.  CONT
**$         rad  geofac  wfrac  skin
GEOMETRY  K  0.5  1.  1.  0.
PERF  TUBE-END  'INJECTOR 4'
**$ UBA    ff  Status  Connection
   4 1 1  1.  OPEN    FLOW-FROM  'SURFACE'
** **
** **
WELL  'INJECTOR 5'
                  ** mole fraction of water (steam) injected
INJECTOR MOBWEIGHT EXPLICIT 'INJECTOR 5'
INCOMP  WATER-GAS  0.75  0.  0.  0.  0.25
TINJW  337.
QUAL  0.9
OPERATE  MAX  BHP  150.  CONT
**$         rad  geofac  wfrac  skin
GEOMETRY  K  0.5  1.  1.  0.
PERF  TUBE-END  'INJECTOR 5'
**$ UBA    ff  Status  Connection
   5 1 1  1.  OPEN    FLOW-FROM  'SURFACE'
** **
** **
WELL  'INJECTOR 6'
                  ** mole fraction of water (steam) injected
INJECTOR MOBWEIGHT EXPLICIT 'INJECTOR 6'
INCOMP  WATER-GAS  0.75  0.  0.  0.  0.25
TINJW  337.
QUAL  0.9
OPERATE  MAX  BHP  150.  CONT
**$         rad  geofac  wfrac  skin
GEOMETRY  K  0.5  1.  1.  0.
PERF  TUBE-END  'INJECTOR 6'
**$ UBA    ff  Status  Connection
   6 1 1  1.  OPEN    FLOW-FROM  'SURFACE'
** **
** **
WELL  'INJECTOR 7'
                  ** mole fraction of water (steam) injected
INJECTOR MOBWEIGHT EXPLICIT 'INJECTOR 7'
INCOMP  WATER-GAS  0.75  0.  0.  0.  0.25
TINJW  337.
QUAL  0.9
OPERATE  MAX  BHP  150.  CONT
**$         rad  geofac  wfrac  skin
GEOMETRY  K  0.5  1.  1.  0.
PERF  TUBE-END  'INJECTOR 7'
**$ UBA    ff  Status  Connection
```

```
   7 1 1  1.  OPEN    FLOW-FROM  'SURFACE'
** **
** **
WELL  'INJECTOR 8'
                ** mole fraction of water (steam) injected
INJECTOR MOBWEIGHT EXPLICIT 'INJECTOR 8'
INCOMP  WATER-GAS  0.75  0.  0.  0.  0.25
TINJW  337.
QUAL  0.9
OPERATE  MAX  BHP  150.  CONT
**$        rad  geofac  wfrac  skin
GEOMETRY  K  0.5  1.  1.  0.
PERF  TUBE-END  'INJECTOR 8'
**$ UBA    ff  Status  Connection
   8 1 1  1.  OPEN    FLOW-FROM  'SURFACE'
** **
** **
WELL  'INJECTOR 9'
                ** mole fraction of water (steam) injected
INJECTOR MOBWEIGHT EXPLICIT 'INJECTOR 9'
INCOMP  WATER-GAS  0.75  0.  0.  0.  0.25
TINJW  337.
QUAL  0.9
OPERATE  MAX  BHP  150.  CONT
**$        rad  geofac  wfrac  skin
GEOMETRY  K  0.5  1.  1.  0.
PERF  TUBE-END  'INJECTOR 9'
**$ UBA    ff  Status  Connection
   9 1 1  1.  OPEN    FLOW-FROM  'SURFACE'
** **
** **
WELL  'INJECTOR 10'
                ** mole fraction of water (steam) injected
INJECTOR MOBWEIGHT EXPLICIT 'INJECTOR 10'
INCOMP  WATER-GAS  0.75  0.  0.  0.  0.25
TINJW  337.
QUAL  0.9
OPERATE  MAX  BHP  150.  CONT
**$        rad  geofac  wfrac  skin
GEOMETRY  K  0.5  1.  1.  0.
PERF  TUBE-END  'INJECTOR 10'
**$ UBA     ff  Status  Connection
   10 1 1  1.  OPEN    FLOW-FROM  'SURFACE'
** **
** **
WELL 11  'INJECTOR 11'
                ** mole fraction of water (steam) injected
INJECTOR MOBWEIGHT 'INJECTOR 11'
INCOMP  WATER-Gas  0.75 0.0 0.0 0.0 0.25
TINJW 337
QUAL  0.9
OPERATE  MAX  BHP 150  CONT
*GEOMETRY *K 0.50 1 1 0
*PERF *TUBE-END 'INJECTOR 11'
    11 1 1 1.00
**
**
```

```
WELL 12 'PRODUCER 1'
PRODUCER 'PRODUCER 1'
OPERATE  MIN  BHP  132  CONT REPEAT
                  ** i  j  k
**$       rad  geofac  wfrac  skin
GEOMETRY  K  0.5  1.  1.  0.
PERF  TUBE-END  'PRODUCER 1'
**$ UBA    ff  Status  Connection
  1 1 50  1.  OPEN    FLOW-TO  'SURFACE'
** **
** **
WELL 13 'PRODUCER 2'
PRODUCER 'PRODUCER 2'
OPERATE  MIN  BHP  132  CONT REPEAT
                  ** i  j  k
**$       rad  geofac  wfrac  skin
GEOMETRY  K  0.5  1.  1.  0.
PERF  TUBE-END  'PRODUCER 2'
**$ UBA    ff  Status  Connection
  2 1 50  1.  OPEN    FLOW-TO  'SURFACE'
** **
** **
WELL 14 'PRODUCER 3'
PRODUCER 'PRODUCER 3'
OPERATE  MIN  BHP  132  CONT REPEAT
                  ** i  j  k
**$       rad  geofac  wfrac  skin
GEOMETRY  K  0.5  1.  1.  0.
PERF  TUBE-END  'PRODUCER 3'
**$ UBA    ff  Status  Connection
  3 1 50  1.  OPEN    FLOW-TO  'SURFACE'
** **
** **
WELL 15 'PRODUCER 4'
PRODUCER 'PRODUCER 4'
OPERATE  MIN  BHP  132  CONT REPEAT
                  ** i  j  k
**$       rad  geofac  wfrac  skin
GEOMETRY  K  0.5  1.  1.  0.
PERF  TUBE-END  'PRODUCER 4'
**$ UBA    ff  Status  Connection
  4 1 50  1.  OPEN    FLOW-TO  'SURFACE'
** **
** **
WELL 16 'PRODUCER 5'
PRODUCER 'PRODUCER 5'
OPERATE  MIN  BHP  132  CONT REPEAT
                  ** i  j  k
**$       rad  geofac  wfrac  skin
GEOMETRY  K  0.5  1.  1.  0.
PERF  TUBE-END  'PRODUCER 5'
**$ UBA    ff  Status  Connection
  5 1 50  1.  OPEN    FLOW-TO  'SURFACE'
** **
** **
WELL 17 'PRODUCER 6'
PRODUCER 'PRODUCER 6'
```

```
OPERATE  MIN  BHP  132  CONT REPEAT
                  ** i  j  k
**$        rad  geofac  wfrac  skin
GEOMETRY  K  0.5  1.  1.  0.
PERF  TUBE-END  'PRODUCER 6'
**$ UBA     ff  Status  Connection
   6 1 50  1.  OPEN    FLOW-TO  'SURFACE'
** **
** **

WELL 18 'PRODUCER 7'
PRODUCER 'PRODUCER 7'
OPERATE  MIN  BHP  132  CONT REPEAT
                  ** i  j  k
**$        rad  geofac  wfrac  skin
GEOMETRY  K  0.5  1.  1.  0.
PERF  TUBE-END  'PRODUCER 7'
**$ UBA     ff  Status  Connection
   7 1 50  1.  OPEN    FLOW-TO  'SURFACE'
** **
** **
WELL 19 'PRODUCER 8'
PRODUCER 'PRODUCER 8'
OPERATE  MIN  BHP  132  CONT REPEAT
                  ** i  j  k
**$        rad  geofac  wfrac  skin
GEOMETRY  K  0.5  1.  1.  0.
PERF  TUBE-END  'PRODUCER 8'
**$ UBA     ff  Status  Connection
   8 1 50  1.  OPEN    FLOW-TO  'SURFACE'
** **
** **
WELL 20 'PRODUCER 9'
PRODUCER 'PRODUCER 9'
OPERATE  MIN  BHP  132  CONT REPEAT
                  ** i  j  k
**$        rad  geofac  wfrac  skin
GEOMETRY  K  0.5  1.  1.  0.
PERF  TUBE-END  'PRODUCER 9'
**$ UBA     ff  Status  Connection
   9 1 50  1.  OPEN    FLOW-TO  'SURFACE'
** **
** **
WELL 21 'PRODUCER 10'
PRODUCER 'PRODUCER 10'
OPERATE  MIN  BHP  132  CONT REPEAT
                  ** i  j  k
**$        rad  geofac  wfrac  skin
GEOMETRY  K  0.5  1.  1.  0.
PERF  TUBE-END  'PRODUCER 10'
**$ UBA      ff  Status  Connection
   10 1 50  1.  OPEN    FLOW-TO  'SURFACE'
** **    well 22 'PRODUCER 11'
** **
WELL 22 'PRODUCER 11'
PRODUCER 'PRODUCER 11'
OPERATE  MIN  BHP  132  CONT REPEAT
```

```
                    ** i  j  k
**$        rad  geofac  wfrac  skin
GEOMETRY  K  0.5  1.  1.  0.
PERF  TUBE-END  'PRODUCER 11'
**$ UBA      ff  Status  Connection
   11 1 50  1.  OPEN    FLOW-TO  'SURFACE'

**
*TIME 1
*TIME 2
*TIME 3
*TIME 4
*TIME 5
*TIME 6
*TIME 7
*TIME 8
*TIME 9
*TIME 10
*TIME 11
*TIME 12
*TIME 13
*TIME 14
*TIME 15
*TIME 16
*TIME 17
*TIME 18
*TIME 19
*TIME 20
*TIME 21
*TIME 22
*TIME 23
*TIME 24
*TIME 25
*TIME 26
*TIME 27
*TIME 28
*TIME 29
*TIME 30
*TIME 40
*TIME 50
*TIME 60
*TIME 70
*TIME 150
*TIME 300
*STOP
```

A.3. Steam/CO_2 Base Case Model

```
**----------------------INPUT-OUTPUT CONTROL-----------------------------------------
*INUNIT *field
*OUTUNIT *field
**-------------------------RESERVOIR DESCRIPTION-----------------------------------
*GRID *CART 11 1 50
*di *ivar 0.5 0.033 3*0.5 0.033 3*0.5 0.033 0.5
*dj *con 0.5
*dk *con  0.2
*KDIR *DOWN
*POR *con 0.25
*PERMI *con 50
*PERMJ *con 50
*PERMK *IJK 1:11 1 1:50 20
*IJK 2 1 1:50 8000
*IJK 6 1 1:50 8000
*IJK 10 1 1:50 8000
*end-grid
*CPOR 5e-4
*CTPOR 0
*rockcp 35.02
*thconr 106
*thconw 0.36
*thcono 0.077
*thcong 0.0833
**---------------------------COMPONENT PROPERTIES-------------------------------------
*MODEL 5 5 5
*COMPNAME      'WATER'    'HEVY OIL'  'LITE OIL' 'MEDM OIL'                    'CO2'
**             -----      -------               --------  --------          ------
   *CMM        18.02      600           250       450                                 44
   *PCRIT      3206.2     0        225       140               1070
   *TCRIT      705.4      0        800       950               88
   *AVG        1.13e-5    0        5.e-5     1.e-4                       0
   *BVG        1.075      0        0.9       0.9               0
   *MOLDEN     0      0.10113     0.2092     0.1281     0.7848756
   *CP         0      0.000005    0.000015           0         0
   *CT1        0      0.00038     0.00114        0             0
   *CPL1       0      300         132.5      247.5                       35.2
*WATPHASE
*VISCTABLE
**      Temp (F)
       75.0    0.0      40828.8    2.328      10.583      0.0153
      100.0    0.0      13489.8    1.9935     9.061       0.0159
      150.0    0.0      1092.4     1.4905     6.775       0.0163
      200.0    0.0      130.3      1.1403     5.183       0.0136
      250.0    0.0      60.6       0.8896     4.0434      0.0115
      300.0    0.0      31         0.7058     3.2082      0.0123
      350.0    0.0      17.9       0.5683     2.5833      0.0131
      400      0        10         0.4754     2.0383              0.0142
           450      0       6                       0.4053     1.5765         0.0151
*OILPHASE
*VISCTABLE
**      Temp (F)
```

```
      75.0    40828.8     40828.8    2.328     10.583      0.0154
      100.0   13489.8     13489.8    1.9935    9.061       0.0161
      150.0   1092.4      1092.4     1.4905    6.775       0.0174
      200.0   130.3       130.3      1.1403    5.183       0.0187
      250.0   60.6        60.6       0.8896    4.0434      0.02
      300.0   31          31         0.7058    3.2082      0.0212
      350.0   17.9        17.9       0.5683    2.5833      0.0223
      400     10          10         0.4754    2.0383              0.0232
            450    6         6           0.4053    1.5765         0.0244
*GASLIQKV
 *KVTABLIM    1.2850E+02    1.6350E+02    1.5000E+02    7.0000E+02    ** low/high pressure; low/high temperature
 *KVTABLE 'MEDM OIL'
 **           Pressure,   psia
 ** T, deg F   1.2850E+02 1.3350E+02 1.3850E+02 1.4350E+02 1.4850E+02 1.5350E+02 1.5850E+02 1.6350E+02
 **  150.000
         1.2300E-11 1.2350E-11 1.2418E-11 1.2503E-11 1.2604E-11 1.2721E-11 1.2853E-11 1.3000E-11
 **  200.000
         4.2382E-10 4.2209E-10 4.2095E-10 4.2037E-10 4.2030E-10 4.2070E-10 4.2156E-10 4.2283E-10
 **  250.000  <extrap.>  <extrap.>  <extrap.>  <extrap.>  <extrap.>  <extrap.>  <extrap.>  <extrap.>
         8.3533E-10 8.3183E-10 8.2949E-10 8.2824E-10 8.2799E-10 8.2869E-10 8.3026E-10 8.3266E-10
 **  300.000  <extrap.>  <extrap.>  <extrap.>  <extrap.>  <extrap.>  <extrap.>  <extrap.>  <extrap.>
         1.2469E-09 1.2416E-09 1.2380E-09 1.2361E-09 1.2357E-09 1.2367E-09 1.2390E-09 1.2425E-09
 **  350.000                          <extrap.>  <extrap.>  <extrap.>  <extrap.>  <extrap.>
         8.9461E-07 8.7714E-07 8.6123E-07 8.6123E-07 8.6123E-07 8.6123E-07 8.6123E-07 8.6123E-07
 **  400.000
         5.8011E-06 5.6720E-06 5.5536E-06 5.4448E-06 5.3446E-06 5.2523E-06 5.1670E-06 5.0882E-06
 **  450.000
         2.9574E-05 2.8854E-05 2.8191E-05 2.7579E-05 2.7013E-05 2.6489E-05 2.6002E-05 2.5550E-05
 **  500.000
         1.2397E-04 1.2076E-04 1.1779E-04 1.1504E-04 1.1250E-04 1.1013E-04 1.0793E-04 1.0588E-04
 **  550.000
         4.4313E-04 4.3112E-04 4.2002E-04 4.0973E-04 4.0018E-04 3.9129E-04 3.8299E-04 3.7525E-04
 **  600.000
         1.3894E-03 1.3508E-03 1.3150E-03 1.2818E-03 1.2510E-03 1.2222E-03 1.1954E-03 1.1702E-03
 **  650.000
         3.8967E-03 3.7883E-03 3.6877E-03 3.5942E-03 3.5071E-03 3.4257E-03 3.3496E-03 3.2782E-03
 **  700.000
         9.8359E-03 9.5762E-03 9.3340E-03 9.1075E-03 8.8955E-03 8.6967E-03 8.5100E-03 8.3343E-03
 *KVTABLE 'LITE OIL'
 **           Pressure,   psia
 ** T, deg F   1.2850E+02 1.3350E+02 1.3850E+02 1.4350E+02 1.4850E+02 1.5350E+02 1.5850E+02 1.6350E+02
 **  150.000
         3.2209E-06 3.1730E-06 3.1302E-06 3.0921E-06 3.0582E-06 3.0281E-06 3.0016E-06 2.9783E-06
 **  200.000
         2.3993E-05 2.3534E-05 2.3115E-05 2.2734E-05 2.2385E-05 2.2067E-05 2.1777E-05 2.1512E-05
 **  250.000  <extrap.>  <extrap.>  <extrap.>  <extrap.>  <extrap.>  <extrap.>  <extrap.>  <extrap.>
         4.4765E-05 4.3894E-05 4.3100E-05 4.2375E-05 4.1713E-05 4.1107E-05 4.0552E-05 4.0045E-05
 **  300.000  <extrap.>  <extrap.>  <extrap.>  <extrap.>  <extrap.>  <extrap.>  <extrap.>  <extrap.>
         6.5537E-05 6.4255E-05 6.3085E-05 6.2017E-05 6.1040E-05 6.0146E-05 5.9328E-05 5.8578E-05
 **  350.000                          <extrap.>  <extrap.>  <extrap.>  <extrap.>  <extrap.>
         1.8104E-03 1.7594E-03 1.7124E-03 1.7124E-03 1.7124E-03 1.7124E-03 1.7124E-03 1.7124E-03
 **  400.000
         5.1820E-03 5.0293E-03 4.8878E-03 4.7566E-03 4.6345E-03 4.5207E-03 4.4143E-03 4.3148E-03
 **  450.000
         1.2891E-02 1.2497E-02 1.2133E-02 1.1794E-02 1.1479E-02 1.1185E-02 1.0910E-02 1.0652E-02
 **  500.000
         2.8590E-02 2.7694E-02 2.6864E-02 2.6093E-02 2.5375E-02 2.4705E-02 2.4077E-02 2.3489E-02
```

```
** 550.000
        5.7696E-02 5.5856E-02 5.4150E-02 5.2564E-02 5.1087E-02 4.9707E-02 4.8415E-02 4.7204E-02
** 600.000
        1.0763E-01 1.0416E-01 1.0094E-01 9.7951E-02 9.5162E-02 9.2556E-02 9.0116E-02 8.7827E-02
** 650.000
        1.8762E-01 1.8156E-01 1.7594E-01 1.7071E-01 1.6584E-01 1.6128E-01 1.5701E-01 1.5300E-01
** 700.000
        3.0700E-01 2.9724E-01 2.8817E-01 2.7972E-01 2.7183E-01 2.6445E-01 2.5753E-01 2.5102E-01
*KVTABLE 'CO2    '
**          Pressure,   psia
** T, deg F   1.2850E+02 1.3350E+02 1.3850E+02 1.4350E+02 1.4850E+02 1.5350E+02 1.5850E+02 1.6350E+02
** 150.000
        4.2077E+02 4.0551E+02 3.9134E+02 3.7816E+02 3.6587E+02 3.5438E+02 3.4362E+02 3.3351E+02
** 200.000
        5.5985E+02 5.3950E+02 5.2061E+02 5.0303E+02 4.8663E+02 4.7130E+02 4.5693E+02 4.4343E+02
** 250.000  <extrap.> <extrap.> <extrap.> <extrap.> <extrap.> <extrap.> <extrap.> <extrap.>
        6.9892E+02 6.7349E+02 6.4988E+02 6.2790E+02 6.0739E+02 5.8821E+02 5.7023E+02 5.5335E+02
** 300.000  <extrap.> <extrap.> <extrap.> <extrap.> <extrap.> <extrap.> <extrap.> <extrap.>
        8.3800E+02 8.0748E+02 7.7914E+02 7.5277E+02 7.2815E+02 7.0512E+02 6.8354E+02 6.6326E+02
** 350.000  <extrap.> <extrap.> <extrap.> <extrap.> <extrap.> <extrap.> <extrap.> <extrap.>
        9.7707E+02 9.4147E+02 9.0841E+02 8.7764E+02 8.4891E+02 8.2204E+02 7.9685E+02 7.7318E+02
** 400.000  <extrap.> <extrap.> <extrap.> <extrap.> <extrap.> <extrap.> <extrap.> <extrap.>
        1.1161E+03 1.0755E+03 1.0377E+03 1.0025E+03 9.6967E+02 9.3895E+02 9.1015E+02 8.8310E+02
** 450.000  <extrap.> <extrap.> <extrap.> <extrap.> <extrap.> <extrap.> <extrap.> <extrap.>
        1.2552E+03 1.2095E+03 1.1669E+03 1.1274E+03 1.0904E+03 1.0559E+03 1.0235E+03 9.9301E+02
** 500.000  <extrap.> <extrap.> <extrap.> <extrap.> <extrap.> <extrap.> <extrap.> <extrap.>
        1.3943E+03 1.3434E+03 1.2962E+03 1.2522E+03 1.2112E+03 1.1728E+03 1.1368E+03 1.1029E+03
** 550.000  <extrap.> <extrap.> <extrap.> <extrap.> <extrap.> <extrap.> <extrap.> <extrap.>
        1.5334E+03 1.4774E+03 1.4255E+03 1.3771E+03 1.3319E+03 1.2897E+03 1.2501E+03 1.2128E+03
** 600.000  <extrap.> <extrap.> <extrap.> <extrap.> <extrap.> <extrap.> <extrap.> <extrap.>
        1.6724E+03 1.6114E+03 1.5547E+03 1.5020E+03 1.4527E+03 1.4066E+03 1.3634E+03 1.3228E+03
** 650.000  <extrap.> <extrap.> <extrap.> <extrap.> <extrap.> <extrap.> <extrap.> <extrap.>
        1.8115E+03 1.7454E+03 1.6840E+03 1.6268E+03 1.5735E+03 1.5235E+03 1.4767E+03 1.4327E+03
** 700.000  <extrap.> <extrap.> <extrap.> <extrap.> <extrap.> <extrap.> <extrap.> <extrap.>
        1.9506E+03 1.8794E+03 1.8133E+03 1.7517E+03 1.6942E+03 1.6404E+03 1.5900E+03 1.5426E+03
*LIQLIQKV
*KVTABLIM    1.2850E+02    1.6350E+02    1.5000E+02    7.0000E+02    ** low/high pressure; low/high temperature
*KVTABLE 'CO2    '
**          Pressure,   psia
** T, deg F   1.2850E+02 1.3350E+02 1.3850E+02 1.4350E+02 1.4850E+02 1.5350E+02 1.5850E+02 1.6350E+02
** 150.000
        2.8003E+01 2.7994E+01 2.7985E+01 2.7976E+01 2.7967E+01 2.7958E+01 2.7949E+01 2.7940E+01
** 200.000
        3.0849E+01 3.0838E+01 3.0827E+01 3.0816E+01 3.0805E+01 3.0794E+01 3.0783E+01 3.0772E+01
** 250.000
        3.1034E+01 3.1021E+01 3.1009E+01 3.0996E+01 3.0983E+01 3.0971E+01 3.0958E+01 3.0945E+01
** 300.000
        2.9329E+01 2.9315E+01 2.9301E+01 2.9287E+01 2.9273E+01 2.9259E+01 2.9245E+01 2.9231E+01
** 350.000  <extrap.> <extrap.> <extrap.>
        2.7718E+01 2.7703E+01 2.7688E+01 2.6530E+01 2.6515E+01 2.6500E+01 2.6485E+01 2.6470E+01
** 400.000  <extrap.> <extrap.> <extrap.> <extrap.> <extrap.> <extrap.> <extrap.> <extrap.>
        2.6195E+01 2.6179E+01 2.6163E+01 2.4032E+01 2.4017E+01 2.4001E+01 2.3985E+01 2.3970E+01
** 450.000  <extrap.> <extrap.> <extrap.> <extrap.> <extrap.> <extrap.> <extrap.> <extrap.>
        2.4756E+01 2.4739E+01 2.4722E+01 2.1770E+01 2.1754E+01 2.1738E+01 2.1722E+01 2.1706E+01
** 500.000  <extrap.> <extrap.> <extrap.> <extrap.> <extrap.> <extrap.> <extrap.> <extrap.>
        2.3396E+01 2.3378E+01 2.3361E+01 1.9720E+01 1.9704E+01 1.9688E+01 1.9671E+01 1.9655E+01
** 550.000  <extrap.> <extrap.> <extrap.> <extrap.> <extrap.> <extrap.> <extrap.> <extrap.>
```

2.2111E+01 2.2093E+01 2.2075E+01 1.7864E+01 1.7847E+01 1.7831E+01 1.7815E+01 1.7799E+01
** 600.000 <extrap.> <extrap.> <extrap.> <extrap.> <extrap.> <extrap.> <extrap.> <extrap.>
2.0896E+01 2.0877E+01 2.0859E+01 1.6182E+01 1.6166E+01 1.6150E+01 1.6133E+01 1.6117E+01
** 650.000 <extrap.> <extrap.> <extrap.> <extrap.> <extrap.> <extrap.> <extrap.> <extrap.>
1.9748E+01 1.9729E+01 1.9710E+01 1.4659E+01 1.4643E+01 1.4627E+01 1.4611E+01 1.4595E+01
** 700.000 <extrap.> <extrap.> <extrap.> <extrap.> <extrap.> <extrap.> <extrap.> <extrap.>
1.8663E+01 1.8644E+01 1.8625E+01 1.3279E+01 1.3263E+01 1.3247E+01 1.3232E+01 1.3216E+01

**----------ROCK~FLUID DATA----------

*rockfluid

RPT 1

*swt ** Water-oil relative permeabilities

** Sw	krw	kro	Pcow
0	0	0.87	24
0.027777778	5.95E-07	0.821703443	16
0.097222222	8.93E-05	0.702354595	5.8
0.166666667	0.000771605	0.587384259	4.8
0.236111111	0.00310789	0.479366126	3.2
0.305555556	0.008716873	0.380388285	2.7
0.375	0.019775391	0.292053223	2.3
0.444444444	0.039018442	0.215477824	2.1
0.513888889	0.069739192	0.15129337	1.9
0.583333333	0.115788966	0.099645544	1.8
0.652777778	0.181577255	0.060194423	1.5
0.722222222	0.272071712	0.032114483	1
0.791666667	0.392798153	0.0140946	0
0.861111111	0.549840559	0.004338045	0
0.930555556	0.749841072	0.000562489	0
1	1	0	0

*slt ** Oil-gas relative permeabilities

** Sl	Krg	Krog	Pcog
0.34	1	0	0
0.4	0.826	0.008	0
0.45	0.694	0.028	0
0.5	0.574	0.059	0
0.55	0.465	0.101	0
0.6	0.367	0.155	0
0.65	0.281	0.221	0
0.7	0.207	0.298	0
0.75	0.143	0.386	0
0.8	0.092	0.486	0
0.85	0.052	0.597	0
0.9	0.023	0.72	0
0.95	0.006	0.79	0
1	0	0.87	0

**----------INITIAL CONDIRION----------

*initial

VERTICAL DEPTH_AVE

INITREGION 1

REFPRES 132

REFBLOCK 1 1 50

*sw *con 0.28

*so *con 0.72

*temp *con 150.

*mfrac_oil 'LITE OIL' *con 0.01

*mfrac_oil 'MEDM OIL' *con 0.02

*mfrac_oil 'HEVY OIL' *con 0.97

```
**-----------------------------------NUMERICAL CONTROL----------------------------------------
*NUMERICAL
*RUN
**-----------------------------------RECURRENT DATA-------------------------------------------
time 0
DTWELL 0.05
**
**
WELL 1  'INJECTOR 1'
                ** mole fraction of water (steam) injected
INJECTOR MOBWEIGHT 'INJECTOR 1'
INCOMP  WATER  0.75  0.0 0.0 0.0 0.25
TINJW 337
QUAL  0.9
OPERATE  MAX  BHP 150  CONT
*GEOMETRY *K 0.50 1 1 0
*PERF *TUBE-END 'INJECTOR 1'
    1 1 1 1.00
**
**
WELL 2  'INJECTOR 2'
                ** mole fraction of water (steam) injected
INJECTOR MOBWEIGHT 'INJECTOR 2'
INCOMP  WATER  0.75  0.0 0.0 0.0 0.25
TINJW 337
QUAL  0.9
OPERATE  MAX  BHP 150  CONT
*GEOMETRY *K 0.50 1 1 0
*PERF *TUBE-END 'INJECTOR 2'
    2 1 1 1.00
**
**
WELL 3  'INJECTOR 3'
                ** mole fraction of water (steam) injected
INJECTOR MOBWEIGHT 'INJECTOR 3'
INCOMP  WATER  0.75  0.0 0.0 0.0 0.25
TINJW 337
QUAL  0.9
OPERATE  MAX  BHP 150  CONT
*GEOMETRY *K 0.50 1 1 0
*PERF *TUBE-END 'INJECTOR 3'
    3 1 1 1.00
**
**
WELL 4  'INJECTOR 4'
                ** mole fraction of water (steam) injected
INJECTOR MOBWEIGHT 'INJECTOR 4'
INCOMP  WATER  0.75  0.0 0.0 0.0 0.25
TINJW 337
QUAL  0.9
OPERATE  MAX  BHP 150  CONT
*GEOMETRY *K 0.50 1 1 0
*PERF *TUBE-END 'INJECTOR 4'
    4 1 1 1.00
**
**
WELL 5  'INJECTOR 5'
```

```
                ** mole fraction of water (steam) injected
INJECTOR MOBWEIGHT 'INJECTOR 5'
INCOMP  WATER  0.75  0.0 0.0 0.0 0.25
TINJW 337
QUAL  0.9
OPERATE  MAX  BHP 150  CONT
*GEOMETRY *K 0.50 1 1 0
*PERF *TUBE-END 'INJECTOR 5'
    5 1 1 1.00
**
**
WELL 6  'INJECTOR 6'
                ** mole fraction of water (steam) injected
INJECTOR MOBWEIGHT 'INJECTOR 6'
INCOMP  WATER  0.75  0.0 0.0 0.0 0.25
TINJW 337
QUAL  0.9
OPERATE  MAX  BHP 150  CONT
*GEOMETRY *K 0.50 1 1 0
*PERF *TUBE-END 'INJECTOR 6'
    6 1 1 1.00
**
**
WELL 7  'INJECTOR 7'
                ** mole fraction of water (steam) injected
INJECTOR MOBWEIGHT 'INJECTOR 7'
INCOMP  WATER  0.75  0.0 0.0 0.0 0.25
TINJW 337
QUAL  0.9
OPERATE  MAX  BHP 150  CONT
*GEOMETRY *K 0.50 1 1 0
*PERF *TUBE-END 'INJECTOR 7'
    7 1 1 1.00
**
**
WELL 8  'INJECTOR 8'
                ** mole fraction of water (steam) injected
INJECTOR MOBWEIGHT 'INJECTOR 8'
INCOMP  WATER  0.75  0.0 0.0 0.0 0.25
TINJW 337
QUAL  0.9
OPERATE  MAX  BHP 150  CONT
*GEOMETRY *K 0.50 1 1 0
*PERF *TUBE-END 'INJECTOR 8'
    8 1 1 1.00
**
**
WELL 9  'INJECTOR 9'
                ** mole fraction of water (steam) injected
INJECTOR MOBWEIGHT 'INJECTOR 9'
INCOMP  WATER  0.75  0.0 0.0 0.0 0.25
TINJW 337
QUAL  0.9
OPERATE  MAX  BHP 150  CONT
*GEOMETRY *K 0.50 1 1 0
*PERF *TUBE-END 'INJECTOR 9'
    9 1 1 1.00
```

```
**
**
WELL 10  'INJECTOR 10'
                ** mole fraction of water (steam) injected
INJECTOR MOBWEIGHT 'INJECTOR 10'
INCOMP  WATER  0.75  0.0 0.0 0.0 0.25
TINJW 337
QUAL  0.9
OPERATE  MAX  BHP 150  CONT
*GEOMETRY *K 0.50 1 1 0
*PERF *TUBE-END 'INJECTOR 10'
    10 1 1 1.00
**
**
WELL 11  'INJECTOR 11'
                ** mole fraction of water (steam) injected
INJECTOR MOBWEIGHT 'INJECTOR 11'
INCOMP  WATER  0.75  0.0 0.0 0.0 0.25
TINJW 337
QUAL  0.9
OPERATE  MAX  BHP 150  CONT
*GEOMETRY *K 0.50 1 1 0
*PERF *TUBE-END 'INJECTOR 11'
    11 1 1 1.00
**
**
WELL 12 'PRODUCER 1'
PRODUCER 'PRODUCER 1'
OPERATE  MIN  BHP  132  CONT REPEAT
                ** i  j  k
**$        rad  geofac  wfrac  skin
*GEOMETRY *K 0.50 1 1 0
*PERF *TUBE-END 'PRODUCER 1'
    1 1 50 1.00
**
**
WELL 13 'PRODUCER 2'
PRODUCER 'PRODUCER 2'
OPERATE  MIN  BHP  132  CONT REPEAT
                ** i  j  k
**$        rad  geofac  wfrac  skin
*GEOMETRY *K 0.50 1 1 0
*PERF *TUBE-END 'PRODUCER 2'
    2 1 50 1.00
**
**
WELL 14 'PRODUCER 3'
PRODUCER 'PRODUCER 3'
OPERATE  MIN  BHP  132  CONT REPEAT
                ** i  j  k
**$        rad  geofac  wfrac  skin
*GEOMETRY *K 0.50 1 1 0
*PERF *TUBE-END 'PRODUCER 3'
    3 1 50 1.00
**
**
WELL 15 'PRODUCER 4'
```

```
PRODUCER 'PRODUCER 4'
OPERATE  MIN  BHP  132  CONT REPEAT
                    ** i  j  k
**$         rad  geofac  wfrac  skin
*GEOMETRY *K 0.50 1 1 0
*PERF *TUBE-END 'PRODUCER 4'
    4 1 50 1.00
**
**
WELL 16 'PRODUCER 5'
PRODUCER 'PRODUCER 5'
OPERATE  MIN  BHP  132  CONT REPEAT
                    ** i  j  k
**$         rad  geofac  wfrac  skin
*GEOMETRY *K 0.50 1 1 0
*PERF *TUBE-END 'PRODUCER 5'
    5 1 50 1.00
**
**
WELL 17 'PRODUCER 6'
PRODUCER 'PRODUCER 6'
OPERATE  MIN  BHP  132  CONT REPEAT
                    ** i  j  k
**$         rad  geofac  wfrac  skin
*GEOMETRY *K 0.50 1 1 0
*PERF *TUBE-END 'PRODUCER 6'
    6 1 50 1.00
**
**
WELL 18 'PRODUCER 7'
PRODUCER 'PRODUCER 7'
OPERATE  MIN  BHP  132  CONT REPEAT
                    ** i  j  k
**$         rad  geofac  wfrac  skin
*GEOMETRY *K 0.50 1 1 0
*PERF *TUBE-END 'PRODUCER 7'
    7 1 50 1.00
**
**
WELL 19 'PRODUCER 8'
PRODUCER 'PRODUCER 8'
OPERATE  MIN  BHP  132  CONT REPEAT
                    ** i  j  k
**$         rad  geofac  wfrac  skin
*GEOMETRY *K 0.50 1 1 0
*PERF *TUBE-END 'PRODUCER 8'
    8 1 50 1.00
**
**
WELL 20 'PRODUCER 9'
PRODUCER 'PRODUCER 9'
OPERATE  MIN  BHP  132  CONT REPEAT
                    ** i  j  k
**$         rad  geofac  wfrac  skin
*GEOMETRY *K 0.50 1 1 0
*PERF *TUBE-END 'PRODUCER 9'
    9 1 50 1.00
```

```
**
**
WELL 21 'PRODUCER 10'
PRODUCER 'PRODUCER 10'
OPERATE  MIN  BHP  132  CONT REPEAT
                    ** i  j  k
**$        rad  geofac  wfrac  skin
*GEOMETRY *K 0.50 1 1 0
*PERF *TUBE-END 'PRODUCER 10'
    10 1 50 1.00
**
WELL 22 'PRODUCER 11'
PRODUCER 'PRODUCER 11'
OPERATE  MIN  BHP  132  CONT REPEAT
                    ** i  j  k
**$        rad  geofac  wfrac  skin
*GEOMETRY *K 0.50 1 1 0
*PERF *TUBE-END 'PRODUCER 11'
    11 1 50 1.00
**
*TIME 1
*TIME 2
*TIME 3
*TIME 4
*TIME 5
*TIME 6
*TIME 7
*TIME 8
*TIME 9
*TIME 10
*TIME 11
*TIME 12
*TIME 13
*TIME 14
*TIME 15
*TIME 16
*TIME 17
*TIME 18
*TIME 19
*TIME 20
*TIME 21
*TIME 22
*TIME 23
*TIME 24
*TIME 25
*TIME 26
*TIME 27
*TIME 28
*TIME 29
*TIME 30
*TIME 40
*TIME 50
*TIME 60
*TIME 70
*TIME 150
*TIME 300
*STOP
```